REVIEW

Back contacts materials used in thin film CdTe solar cells—A review

Ralph Stephen Hall [iD] | Dan Lamb [iD] | Stuart James Curzon Irvine [iD]

Centre for Solar Energy Research, College of Engineering, Swansea University, St. Asaph, UK

Correspondence
Ralph Stephen Hall, Centre for Solar Energy Research, College of Engineering, Swansea University, St. Asaph, Wales, UK.
Email: r.s.hall@swansea.ac.uk

Funding information
European Regional Development Fund, Grant/Award Number: SPARC II; Engineering and Physical Sciences Research Council, Grant/Award Number: EP/R035997/1

Abstract

CdTe is the leading commercial thin film photovoltaic technology with current record laboratory efficiency (22.1%). However, there is much potential for progress toward the Shockley-Queisser limit (32%). The best CdTe devices have short-circuit current close to the limit but open-circuit voltage has much room for improvement. Back contact optimization is likely to play a key role in any improvement. Back contact material choice is also influenced by their applicability in more complex architectures such as bifacial and tandem solar cells, where high visible and/or near-infrared transparency is required in conjunction with their electrical properties. The CdTe research community has employed many back contact materials and processes to realize them. Excellent reviews of back contacts were published by McCandless and Sites (2011) and Kumar and Rao (2014). There have been numerous publications on CdTe back contacts since 2014. This review includes both recent and older literature to give a comprehensive picture. It includes a categorization of back contact interface materials into groups such as oxides, chalcogenides, pnictides, halides, and organics. The authors attempt to identify the more promising material groups. Attention is drawn to parallels with back contact materials used on other thin film photovoltaics such as perovskites and kesterites.

KEYWORDS

back contacts, CdTe, contact materials, solar cell efficiency, thin film solar cells

1 | INTRODUCTION

Photovoltaics (PV) using thin film CdTe as a photon absorber have been studied for several decades. CdTe was long recognized for its potential to surpass the conversion efficiencies of conventional silicon solar cells based on bandgap matching to the Shockley Queisser limit.[1] However, progress was slow in reaching this protential with best laboratory cell efficiencies climbing from ~9% in 1976 to 16% in 1993.[2,3] A virtual plateau in efficiency followed for the next 20 years

before the efforts of First Solar and GE Global Research (now one entity) helped push the efficiency to 22.1% at the time of this review by the First Solar company.[2,4,5] First Solar are the leading commercial manufacturers of thin film photovoltaics having recently introduced their Series 6 offering in excess of 17% efficiency at the module level.[5,6]
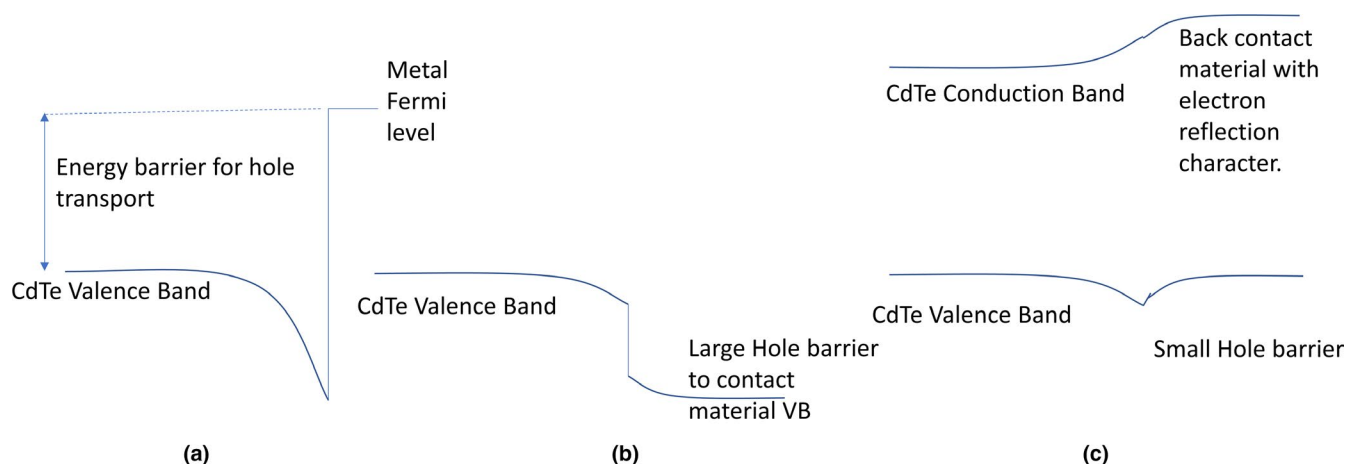
CdTe PV can be constructed under two device architectures (Figure 1); the PV thin films can be deposited onto a substrate material in the general order electrode, p-type CdTe absorber, n-type buffer layer, electrode or the reverse order
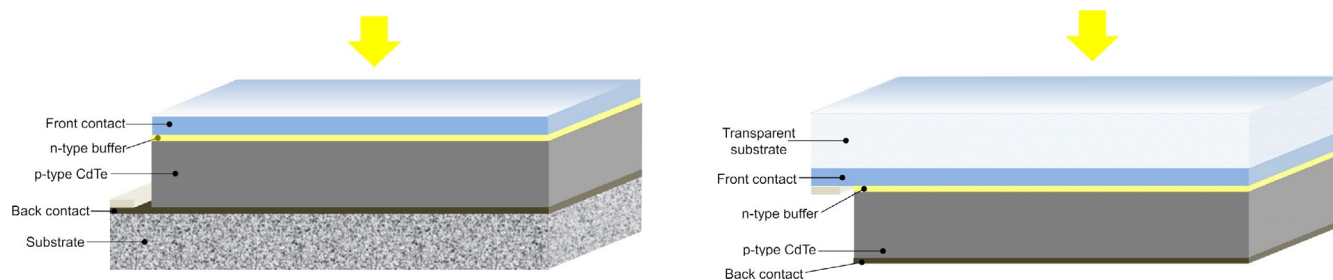
FIGURE 1 Typical superstrate (left) and substrate (right) CdTe solar cells configurations

FIGURE 2 Generalized valence band alignment diagrams for the back contact to CdTe solar cells. (A) To metals—large hole barrier. (B) Generic semiconductor back contact with large hole energy barrier. (C) Generic idealized semiconductor back contact with small hole barrier and electron reflection character

transparent substrate material, transparent electrode, n-type buffer, p-type CdTe absorber, and electrode. The latter is the preferred route for several optimal device performance reasons and necessitates the use of an optically transparent superstrate material and initial electrode layer. The CdTe in superstrate configuration relies on the following factors, among others, to achieve high conversion efficiency. Firstly, a substrate, electrode (front contact), and n-type buffer which are optimized to transmit photons with an energy above the absorber bandgap. Secondly, a chlorine heat treatment of the CdTe and thirdly, an Ohmic (back) contact to the CdTe. The majority of CdTe PV research and all module manufacturing to date has exploited the superstrate configuration.

CdTe has a high electron affinity of around 4.4 eV,[7] which together with its energy gap of around 1.45 eV, means that many materials that might be considered good conductors and thus good back contacts, tend to form Schottky barriers[8] (see Figure 2A) which oppose the flow of current into the solar cell.

The exceptions to this are metals with very high work functions which form Schottky contacts with small barriers and can thus act effectively as Ohmic-like contacts at normal working temperatures (eg, gold and palladium). This

difficulty has been noted many times (eg, Wald (1977),[9] Fahrenbuch (1987)[10]). Demtsu and Sites (2006)[11] gave a good description of how forward-bias rollover can occur due to a rear contact barrier.

Before we consider the multitude of possible back contacts, it is important to note that the chemistry of the materials at and near the back contact needs to be considered as much as the fundamental physical properties of CdTe and its back-interface material. The interface must minimize photogenerated carrier recombination. The simplistic approach of matching the valence band positions through knowledge of a value of the electron affinity and the bandgap, although useful, can also be misleading if the chemistry leads to interlayer compound formation, or interfacial states lead to Fermi level pinning.[12]

The back contact issue is not unique to CdTe—it is also believed to be a limiting factor in some other thin film solar cell technologies; such as the perovskite structure materials ("ABX_3" which achieve high efficiency but are not yet a well-established commercial technology), and other thin film solar cell technologies using chalcogenides (mainly CIGS and kesterites[13,14]). The back contact is also commonly referred to as the hole transport material (HTM) in perovskites

and is one factor limiting both efficiency and long-term stability[15] of perovskite devices.

Many CdTe back contact technologies utilize small amounts of copper to increase the p-type doping level. This element can be delivered as a metal layer with a thickness of a few nanometers, or as a copper compound, such as Cu_xTe. Thicknesses of copper-containing layers is often well below 10 nm. However, it is known that as well as providing p-type doping copper introduces deep levels[16] into the CdTe, and that copper is highly soluble in CdTe.[17] Copper re-distribution within a polycrystalline solar cell is a complex process. However, the record efficiency cells have almost unanimously utilized copper as part of their back contact technology.

The challenge of creating an optimum back-surface contact for CdTe has been a goal of many research teams for decades and has been reviewed before, for example by McCandless and Sites (2011)[18] and Kumar and Rao (2014).[19] This review seeks to integrate post-2014 literature into a comprehensive view of the subject.

Back contact technologies for polycrystalline CdTe on flexible substrates have recently been reviewed by Znajdek et al (2019).[20] A small number of back contact technologies were reviewed in this paper, before copper, molybdenum, and silver (full coverage of silver and a mesh) were used in bending test experiments. In the case of flexible cells, adhesion and matching of thermal expansion coefficients are even more crucial than when CdTe is deposited on rigid substrates.

In reviewing the literature for back contacts to CdTe, it seemed prudent to the authors to group the many materials that have been used into categories. However, it is acknowledged that the categorization used here is not unique. Neither does it adequately describe the multiple materials and processes used in many cases. Nevertheless, it can be a useful approach. The list of categories used is given in Table 1.

In this analysis, it is often difficult to do like-for-like comparisons. Devices with deliberately grown Cd(Se,Te) absorbers will have a different point at which solar cell performance is strongly limited by the back contact, due to effects such as different front contact, carrier lifetimes, and grain boundary passivation. Consequently, such devices are largely excluded from the analysis, except when little or no information is available for a back contact material with a CdTe absorber. CdTe n-type absorber solar cells are not included in this review due to the comparatively little literature available. Differences in the front contact are also present. Often the difference in the front contact will largely affect the short-circuit current. Therefore, power conversion efficiency (PCE), open-circuit voltage (V_{oc}), and fill factor (FF) will be given more consideration.

In some cases, it is arguable as to whether a process treatment also can be classified as a back contact material. One important example is the ubiquitous chlorine heat treatment (CHT) (most commonly using $CdCl_2$ or chlorine diffusion).

TABLE 1 Categories of materials used in back contacts to CdTe solar cells and shorthand notations for the principal components considered within that category

Category	Examples
Group IV	a-Si:H, a-Si$_{1-x}$C$_x$:H, Bi-RGO CuCNi, Cu$_x$Te/SWCNT, graphene:B, SWCNT, graphite
Metal	AgNW/ITO, Cu, Cu NW, Mo
Metal pnictide	MoN$_x$, ZrN, Ni$_2$P
Metal oxide	Cu$_2$O/Au, CuO$_x$ ITO, Cu/Au/ZnO:Al MoO$_3$, MoO$_x$ MoO$_x$:Cu NiO (p-type), V$_2$O$_5$, WO$_3$, ZnO:Al CdO
Metal selenide	VSe$_2$, TiSe$_2$, (BaCuSeF, SrCuSeF)
Metal sulfide	CIS, CIS:N, CuS, CuS/ZnS, FeS$_2$, (Fe,Ni)S$_2$
Metal telluride	Cu$_2$Te, CuTeNi, HgTe:Cu, NiTe$_2$, SnTe/Ni ZnTe:As, ZnTe:Cu, ZnTe:Cu/ITO, ZnTe:N-ITO, ZnTe:Sb
Telluride, other	(N$_2$H$_5$)$_2$CdTe$_2$, Cs$_2$CdTe$_2$, K$_2$CdTe$_2$, Na$_2$CdTe$_2$, As$_2$Te$_3$, Sb$_2$Te$_3$, Bi$_2$Te$_3$
Metal halides and perovskites	CuI, BaCuSeF, SrCuSeF, BaCuSF, BaCuSF/ITO, MAPb(Br$_{1-x}$,I$_x$)$_3$
Organic and carbon containing	CoPC/Au, CuSCN/Au P3HT, PCBM, PEDOT, Pentacene, PFO, Ppy, spiro-OMeTAD

If this treatment leaves the back-surface rich in chlorine, then chlorine can be said to be a constituent of the back contact material, even though a further material will be required for electrical contact.

A second classification of back contact materials is whether the process is free of copper (or other potentially mobile dopants) or not. As mentioned, a small amount of copper has been an integral part of many of the back contact technologies developed for CdTe solar cells. Copper is commonly used to dope CdTe p-type to a suboptimal doping level in the range 10^{14} to 10^{15} cm^{-3}. However, the presence of "excess" copper is also associated with long-term cell degradation.[21] Therefore, many of the copper-containing processes have undergone trials with very restricted amounts of copper to optimize performance, but also to minimize long-term performance drops. Other approaches have sought a copper-free contacting technology.[22] It is not within the scope of this paper to review all the literature on copper usage in back contact technologies, itself the subject of many articles.[23]

A third possible classification is whether the contact material(s) are transparent. (It is noted that CdTe is not transparent in the visible spectrum for absorber layers thick enough to produce high PCE). As shown in Figure 1 the superstrate

configuration transmits photons to the absorber layer via the transparent substrate, front contact, and n-type buffer. However, for some applications such as tandem[24] and bifacial solar cells, a contact with good visible and near-infrared transparency to at least 800 nm is also required. A third technology which requires NIR transparent back contacts is a nonconventional PV-thermal (PVT) solar cell in which the transmitted NIR radiation is used elsewhere, including by focussing NIR onto a heat collector such as an evacuated tube. For these architectures, any use of narrow bandgap materials, or metals thicker than 10 nm or so, at the back surface will reduce substantially transmission of subbandgap radiation through the CdTe. If back contact materials are extremely thin, or do not have close to 100% coverage of the back surface, then a binary transparent/opaque description could be misleading.

The maximum processing temperature during the deposition of back contacts needs to be considered. Although CdTe has a high melting point ($1050°C$[17]), some elements can diffuse quickly through CdTe. In polycrystalline CdTe, diffusion along grain boundaries can be much faster than bulk diffusion (eg, copper[21] and sulfur[25]). Grain boundary passivation from the CHT process can also be affected by loss of Cl[26] at very high subsequent processing temperatures.

The metal(s) used as the final contact also influence PCE in some cases, as well as sometimes making the devices more or less stable over time. This can be through the formation of Schottky barriers or by diffusion into or through the CdTe.

To maximize solar cell PCE, resistive heating losses need to be minimized. If a back contact material has a low lateral conductivity, then a more conductive layer is required on top to avoid excessive series resistance. Conductive materials dominated by hopping conductivity, such as many organic compounds, have very low mobility values compared to relatively large-grained inorganic conductors with delocalized conduction or valence bands. These low mobility materials will always require a more conductive layer on top, or a metal grid/mesh/network with low mean spacing, so lateral transport to a metal is only a short distance.

Although it has been stated that band offsets are of limited use, the concept is of some use in choosing materials to study. Directly measuring band offsets is difficult. XPS studies can give a picture of offsets relative to vacuum level, but less so when buried within a device structure. Analysis of temperature-dependent forward-bias rollover in J-V curves is one method of determining an effective back contact barrier in situ and inferring valence band offset (VBO).

Recently, the concept of initial Fermi level offset (IFLO) has been promoted (Liyanage et al (2019)[27]) through extensive 1-D modeling (using SCAPS[28]); this concept might allow doping levels in CdTe and the back contact material to be accounted in a better manner than just using the VBO.

2 | SURFACE PROCESSING BEFORE BACK CONTACTS DEPOSITION/POST BACK CONTACT DEPOSITION PROCESSING

2.1 | Chemical treatments

Chemical treatments prior to back contact deposition have been reviewed by Kumar and Rao (2014).[19] The as-grown CdTe can be subject to chemical modification by etching prior to back contact deposition. It is noted that the presence of many grain boundaries in polycrystalline CdTe means that some etches which might provide a beneficial surface condition on single-crystal CdTe might increase recombination at grain boundaries on polycrystalline CdTe.

The first etch we mention is an etch using potassium chromate and sulfuric acid (chromate etch) used on p-type bulk-grown CdTe. Anthony et al (1982)[29] measured contact resistances of 0.1-0.5 Ω cm^2 using Cu-Au or Au on a $K_2Cr_2O_7$:H_2SO_4 etched surface—significantly lower than when a bromine-methanol (Br-Me) etch was used. This etch leaves the surface Te-rich with the presence of some TeO_2.[30] Rimmaudo et al (2017)[31] attempted to form a layer of Cu_xTe through a process including Br-Me etching before Cu/Au deposition. The Br-Me etch allowed less Cu to be used, giving a "more optimal" doping and improving device stability. Improved performance was also attributed to the reduction in grain roughness observed in AFM studies. Awni et al (2018)[32] and (2019)[33] also showed grain roughness reduction when using a hydrogen iodide in methanol etch. Additionally, a reduction in back contact barrier height was observed after etching.

Another common etch is a nitric-phosphoric (NP) etch.[34,35] Both Br-Me and NP etches leave the surface Te-rich; the NP etch leaves a thicker Te-rich layer. A Te-rich surface is believed to be beneficial for back contact formation.[36] The NP etch preferentially etches grain boundaries and can be overdone, leading to pinholes. Proskuryakov et al (2007)[37] studied various NP etch conditions using both solar cell J-V characteristics and variable temperature admittance spectroscopy. Short etch times mostly affected the back surface, but longer etch times also caused changes at grain boundaries. Major et al (2014)[38] (Liverpool University) used N-P etches before and after chloride treatments in a study of chloride treatments other than $CdCl_2$ ($MgCl_2$, NaCl, KCl, and $MnCl_2$).

2.2 | Electron reflectors

Hole transport is required at the back contact of a superstrate CdTe solar cell. Electrons which reach the back contact interface are likely to recombine. Hsaio and Sites[39,40] at Colorado State University studied strategies for providing interfaces with an electron reflecting character, reducing interface

recombination. The introduction of a material with a small valence band offset and a larger conduction band (likely higher energy gap) could provide a means for hole transport, while band bending at the interface could lead to an electric field tending to repel electrons from the interface ("reflection"). A generic alignment of conduction and valence bands for an electron reflector back contact is shown in Figure 2C. Hsaio and Sites work suggested that PCE 19%-20% was possible with a 1 μm thick absorber if an electron reflector was used in a structure which also had good optical reflection. ZnTe is an early example of a material with the expected band alignment expected to produce electron reflection when deposited on CdTe. More recently other materials including CdMgTe[41] have been studied as potential electron reflectors.

3 | METAL BACK CONTACTS

Metals tend to form Schottky contacts to p-type CdTe, as indicated by Ponpon (1985)[42] (see Figure 2A). The lowest barriers are formed with high work function metals, nickel (see nickel telluride contacts), and gold, which are a closer match to the electron affinity plus bandgap of CdTe. Gold and platinum are too expensive for use in modules but can be very useful in laboratory studies. Of the economically viable metals, only nickel (and carbon) has work functions sufficiently high to avoid very large Schottky barriers. Nickel in CdTe forms a deep acceptor level.[43] One example paper (Wei Xia et al (2014)[44]) shows the effect of using Ni on as-grown CdTe surfaces: PCE is improved by NP etching before Ni deposition, or by using Te or Te/Cu interlayers before Ni deposition. For long-term stability, the diffusion of metals into CdTe must be considered.

In many cases, tellurides can form at the interface when metals are deposited. The effect of the tellurides on the interface needs to be considered (see also the section on telluride contacts). Even less reactive metals such as gold can form a telluride at the interface. Odkhuu et al (2016)[45] performed electronic structure calculations on the Schottky barriers formed between CdTe and Cu, Pt, and Al when the CdTe surface was Cd-terminated and Te-terminated. Different barrier heights were obtained for the different surface terminations, and barrier heights were found to be heavily influenced by metal-induced gap states. Li et al (2017)[46] also studied Schottky barrier heights for Al, Ag, Au, Cu, and Ni. The lowest Schottky barriers determined were Ni (0.66 eV) and Au (0.44 eV).

4 | TELLURIUM AND TELLURIDE BASED CONTACTS

In this category the following materials that have been used for back contacts will be discussed: tellurium, undoped and doped copper tellurides, mercury telluride, nickel telluride, tin telluride, with a more extensive discussion on zinc telluride and its doping.

4.1 | Tellurium as a back contact

Tellurium is one natural choice of back contact, as the element is already present in the CdTe absorber. The melting point is much lower than CdTe at around 450°C. Tellurium is a (bulk) p-type degenerate semiconductor with reasonably high conductivity that can be increased by doping (copper) and has a low VBO to CdTe.[47]

Niles et al (1996)[48] showed a PCE value of 12.1% with an evaporated Te back contact (V_{oc} 740 mV, J_{sc} 22.4 mA cm^{-2} FF 65.4%), slightly outperforming their control process which involved etching to obtain a Te-rich surface. A near contemporaneous XPS study by Niles et al (1995)[47] had found a valence band offset of 0.26 ± 0.1 eV between the evaporated Te and CdTe. Kraft et al (JAP 2003)[49] found a valence band offset of ~0.5 eV using XPS between CdTe and Te prepared by chemical etching of CdTe. Moffet and Sampath (2017)[50] published XPS characterization work on Te thickness variations on CdTe. Temperature-dependent J-V curves showed the back-barrier height decreasing as Te thickness increased from 2 nm to 8 nm, reaching bulk values at 50 nm.

Tellurium back contacts were one component of the revised structure (Munshi et al (2018)[51] (Colorado State University) used to achieve a cell with 18% PCE They also used a $Mg_xZn_{1-x}O$ buffer, thick CdTe, and front AR coating. The back contact barrier height was suggested by Alfadhili et al (2019)[52] to be smaller for Te than for ZnTe.

Provision of a deposited Te layer has produced higher PCE than a Te-rich layer produced by etching as the Te layer thickness is more controllable in a deposition process, as well as avoiding the possible creation of etched pinholes and affecting passivated grain boundaries.

4.2 | Copper telluride

Copper telluride introduces copper which will dope CdTe[53] and provide the back contact. Ferekides et al (1997)[54] showed PCE values approaching 15%. They found that a thin (50 nm) copper telluride layer produced maximum V_{oc} and FF (best Cu_xTe/Mo back contacted cell: PCE 14.9%, V_{oc} 838 mV, J_{sc} 23.77 mA cm^{-2}, FF 74.95%—NREL certified). McCandless et al (2003)[55] investigated the different phases of copper telluride formed on the back surface following the deposition of different thicknesses of copper. Yan et al (2005)[35] at NREL published on the use of copper telluride. In this case, HgTe was used as well, forming HgCdTe at the back surface, so the role of copper telluride itself is more difficult

to extract. It was also investigated by Avachat (2005)[56] of the University of Central Florida, Wu et al (2007),[57] and Zhou et al (2007)[58] who found that the dominant phase of copper telluride was thickness dependent, becoming more copper rich with increasing thickness. The maximum PCE (12.9%, V_{oc} 797 mV, J_{sc} 22.7 mA cm^{-2}, FF 71.3%, and R_s 1.09 Ω cm^2) was obtained at a copper telluride thickness of 10 nm (mixed CuTe and $Cu_{1.4}Te$ phases), while at a thickness of 60 nm, the PCE dropped to 12.1% (single-phase $Cu_{1.4}Te$). At a thickness of 130 nm, the less thermodynamically stable Cu_2Te phase dominated but V_{oc}, J_{sc}, and FF were all reduced giving a PCE of 7.3%. More recently, Moore (2017)[59] studied combinations of Cu, Te, and carbon paint, all finished with a nickel paint treatment. A representative selection of solar cell parameter results from the literature for copper telluride and tellurium based back contacts is given in Table 2.

Back surface processes that deposit thin layers of copper on Te-rich surfaces also form copper tellurides and, in some cases, the formation of copper tellurides can act as a means of consuming excess copper which could otherwise diffuse through the CdTe. It has also been suggested that copper deposited on top of other layers (specifically ZnTe) can diffuse via grain boundaries to form copper tellurides at the ZnTe-CdTe interface,[60] but the ZnTe is also expected to reduce or slow diffusion of copper into the CdTe.[61]

4.3 | Mercury telluride and $Hg_{1-x}Cd_xTe$

Mercury (II) telluride (HgTe) is a semi-metal rather than a semiconductor. It has a relatively high conductivity compared to CdTe. $Hg_{1-x}Cd_xTe$ alloys are stable with a cubic crystal structure with a nearly constant lattice parameter for all compositions.[17] The low energy gap means that the material is not transparent in the near infrared (NIR) until the Cd composition exceeds around 70%. Hg-Te bonds are relatively weak compared to Cd-Te bonds leading to Hg diffusion at moderately high temperatures.

Janik and Triboulet (1987)[62] showed that HgTe deposited by close space sublimation could provide a low resistance Ohmic contact to CdTe and $Hg_{1-x}Cd_xTe$, due to good work function matching, but did not fabricate solar cells. This work was extended by Zozime and Vermeulin (1988)[63] to analyze specific contact resistance accounting for doping level. Specific contact resistance remained at 15-500 Ω cm^2 for material of resistivity 1.5-45 kΩ cm but dropped to 7 Ω cm^2 for ~70 Ω cm resistivity material.

A paste made of graphite mixed with HgTe (often copper doped) has been used extensively[64,65] and probably was the material used by Britt and Ferekides (1993)[3] in their 15.8% PCE device (V_{oc} 843 mV, J_{sc} 25.1 mA cm^{-2}, FF 74.5%). A CuTe:HgTe doped graphite paste (then silver paste) was used by Wu et al (2001)[66] in NREL's then record 16.5% PCE device (V_{oc} 845 mV, J_{sc} 25.9 mA cm^{-2}, FF 75.5%, this device had cadmium stannate/zinc stannate front contacts).

Hanafusa et al (2001)[67] used a wide range of materials to "dope" graphite pastes used as back contacts. The added materials that resulted in PCE over 12% included the silver halides (AgCl and AgF), silver telluride, silver phosphate and molybdate, as well as nickel phosphide and telluride, and zinc phosphide. Lead-containing additives reduced PCE, as did NiO. Compounds containing Bi and Sb were also tried.

4.4 | Zinc telluride

Zinc telluride (ZnTe) is a semiconductor with an ambient temperature energy gap of around 2.2 eV,[68] higher than the energy gap of CdTe. ZnTe has the same cubic crystal structure as CdTe. The high bandgap means that ZnTe is not suitable for use as a single absorber in a high PCE solar cell. ZnTe can be doped p-type by pnictides (N,[69] P,[70] As,[71] Sb,[72] and Bi) and by copper. The electron affinity of ZnTe is such that the valence band offset to CdTe is very low.[73] This allows hole transport to a metal contact with smaller barriers than for those created by directly contacting CdTe with metals. There are also suggestions that ZnTe could act as an electron reflector if the recombination rate at the interface is sufficiently low (see also section on electron reflectors).

ZnTe was the contact material to CdTe for AMETEK's late 1980s world record ITO/CdS/CdTe/ZnTe/Ni solar cell which achieved PCE 11%. Copper-doped ZnTe on CdTe has been studied since before 1992 (Mondal et al (1992)[74] at the University of Delaware) and by many groups since. By 2015,

TABLE 2 A selection of copper telluride based back contact device results—solar cell parameters including series resistance where known

Reference	Material	V_{oc} (mV)	J_{sc} (mA cm^{-2})	FF (%)	PCE (%)	R_s (Ω scm^2)
Ferekides et al (1997)[54]	CdS/CdTe/Cu$_x$Te/Mo	838	23.8	74.9	14.9	-
Xia et al (2014)[44]	CdS/CdTe/Te/Cu	820	22.2	77.6	14.1	-
Zhou et al (2007)[58]	CdS/CdTe/NP etch/Cu/C-paste/Ag	797	22.7	71.3	12.9	1.09
Kim et al (2018)[236]	ITO/CdS/CdTe/Cu$_2$Te	~800	25.5	59	~12	6.5
Moore (2017)[59]	CdS/CdTe/Cu/Te/Ni	801	22.4	72.4	13.0	1.1
Moore (2017)[59]	MgZnO/CdTe/Cu/Te/Ni	853	25.7	77.9	17.1	0.6

NREL reported a 16.4%[75] PCE, although the focus of this paper was the fact that the CdTe solar cell was flexible.

Amin et al (2002)[76] tried ZnTe and $Cd_{0.5}Zn_{0.5}Te$:N back contacts to thin (1 μm CdTe) solar cells obtaining 8.3% PCE (low FF of 49%) for ZnTe/C:Cu/Ag contacted devices. Chen et al (2019)[77] studied ZnTe:Cu back contacts to CdTe using a CdSe buffer layer (ITO/ZnO/CdSe/CdTe/ZnTe:Cu/Au structure). Although an improvement over the Au only back contact was observed, the maximum PCE was 6.38%.

A ZnTe-based back contact layer still requires metallization. Gessert et al (2014)[78] studied the contact properties of titanium on doped ZnTe. Metal-semiconductor contact resistance is a somewhat neglected area of study in the context of CdTe solar cells (and associated materials): a comprehensive review is overdue but is not within the scope of this article. Gessert et al[78] concluded that the likely range of contact resistance of Ti to ZnTe was 0.1-0.5 Ω cm^2. This is orders of magnitude more than can be achieved with rare metal contacts such as between Au on Pd on $>10^{19}$ cm^{-3} p-doped ZnTe (5×10^{-6} Ω cm^2 – Ozawa et al (1994)[79]).

Kurley et al (2017)[80] used liquid chemistry to modify the rear surface of CdTe solar cells. This approach is categorized here with the ZnTe papers for convenience but is really a distinct approach. The best PCE (12.7%) resulted from forming an interfacial layer of $(N_2H_5)_2CdTe_2$ on top of CdTe. This was a marginal PCE gain over their control device with V_{oc} improved from 684 mV (control) to 726 mV ($(N_2H_5)_2CdTe_2$ treated). Another contact used by Kurley[81] was to spin-coat ZnTe:Sb onto CdTe (best cell PCE 6.4%).

It is clear from Table 3 that in order to obtain high PCE either the back contact process must contain Cu or the CdTe is already heavily p-type doped (Oklobia et al (2019)[71] used arsenic doping).

$Cd_{0.7}Mg_{0.3}Te$ was recently used by Feng et al (2020)[82] to increase the conduction band offset at the back interface while not creating a large VBO. A $Cd_{0.7}Mg_{0.3}Te$ electron reflection layer gave PCE 13.4% (V_{oc} 804 mV, J_{sc} 23.1 mA cm^{-2}, FF 72%) after annealing at an optimum temperature of 425°C. Te/Cu was deposited on the CdMgTe before Au contacts were deposited.

4.5 | Nickel telluride and other transition metal tellurides

Nickel telluride ($NiTe_2$) is a semi-metallic material with intrinsic resistivity 10^{-7} to 10^{-6} Ω cm. It crystallizes with a CdI_2-like structure[83] and is stable even with a few percent tellurium deficiency. Although nickel is a well-used contact metal, studies of $NiTe_2$ are less common. Rotlevi et al (2001)[84] and Dobson et al (2002)[85] published studies of electroless $NiTe_2$ contact formation to CdTe. A PCE of ~10% was obtained (V_{oc} ~ 800 mV, J_{sc} ~ 25 mA cm^{-2}, FF ~ 65%).

Unencapsulated cells were thermally stable to around 200°C, but exposure to water vapor led to reversible degradation.

Other transition metal tellurides have been studied as potential photovoltaic technology materials. There has been little or no experimental work on using them with CdTe absorber solar cells. $MoTe_2$, a layered material,[86] has been numerically modeled as a back contact,[87,88] but we have not found any experimental data on at the time of publication other than the work of Dhar et al (2015)[89] concerning the Mo/CdTe interface and the older work of Löher et al (2000)[90] on MBE-grown CdTe/$MoTe_2$ interfaces.

$MnTe_2$, a p-type semiconductor, was tried by Shen et al (2010)[91] as a back contact in substrate configuration devices. $MnTe_2$ was formed on Mo by annealing of Mn/Te bilayers and by direct evaporation of $MnTe_2$. Devices showed severe forward-bias rollover with V_{oc} limited to about 500 mV.

4.6 | Group IV tellurides

Group IV tellurides are possible materials for back contacts. There are no known experimental studies of silicon telluride (Si_2Te_3) or germanium telluride back contacts and only one numerical study[92] using AMPS software[93] on CdTe solar cells.

Tin (IV) telluride is a narrow gap semiconductor with a rock-salt structure, which might remain in a zinc-blende structure for very thin layers grown on CdTe.[94] Weng et al (2018)[95] experimented on solar cells with eight different contact structures all including a final 100 nm thick Ni layer. Half of the structures included a light NP etch (intended to remove oxides), and half had a longer NP etch (to produce a Te-rich surface). Maximum PCE was obtained with a structure using a light NP etch, 60 nm ZnTe followed by 5 nm of copper then 40 nm SnTe before the metal contact was deposited. This cell gave 14.6% PCE (V_{oc} 841 mV, J_{sc} 24.7 mA cm^{-2}, and FF 70.2%). T. Shu et al (2019)[96] also used SnTe/Ni back contacts (PCE 13.1%, V_{oc} 782 mV, J_{sc} 24.6 mA cm^{-2}, and FF 68%).

Lead telluride (PbTe) has been suggested as a back contact material in 1D simulation studies.[97] XPS has suggested a low VBO between PbTe and CdTe(111) surfaces.[98] It was expected that a two-dimensional electron gas can form at the PbTe/CdTe (111) interface, probably increasing recombination but no experimental solar cell results were available until the work of Swartz et al (2019).[99] They found that despite indications that the CdTe/PbTe:Tl contact was Ohmic, that the PbTe:Tl layer also appeared to be photoconductive. Cells were shunted—limiting the PCE to 9%. The low bandgap of PbTe (~0.29 eV) means that the material is opaque in the NIR and visible bands. Thallium is extremely toxic and not produced in large quantities.

TABLE 3 J-V characteristic parameters for a selection of articles reporting solar cells with ZnTe in the back contact

Reference	back contact	V_{oc} (mV)	J_{sc} (mA cm^{-2})	FF (%)	PCE (%)	Process contains Cu
Mondal et al (1992)[74]	ZnTe:Cu	705	18.8	65.7	8.7	Yes
Mahabaduga et al (2015)[75]	ZnTe:Cu	831	25.5	77.4	16.4	Yes
J. Li et al (2015)[61]	ZnTe:Cu	852	24.3	73.7	15.3	Yes
Kindvall et al (2018)[237]	ZnTe:Cu	804	25.8	62	12.89	Yes
Oklobia et al (2019)[238]	ZnTe:As/Au	696	23.7	72	11.9	No
Kurley (2016)[80,81]	Spin-coated ZnTe:Sb	732	16.1	54.0	6.4	No
Marsillac et al (2007)[239]	ZnTe:N/ITO	550	19.9	52.0	5.7	No
Makhratchev et al (2000)[240]	ZnTe/ZnTe:N/Ni	-	-	-	~10	No?
Avachat (2005)[56]	ZnTe:Cu/ITO/Ni-Al	630	7.7	37.9	3.1	Yes
Ulicna et al (2017)[241]	ZnTe:Cu	727	21.99	70.3	1.25	Yes
Amin et al (2002)[76]	CdTe/ZnTe/C:Cu/Ag	740	22.98	49	8.31	Yes
Amin et al (2002)[76]	CdTe/Cd$_{0.5}$Zn$_{0.5}$Te:N/Au	680	22.6	49	7.46	Yes (?)
Chen et al (2019)[77]	ITO/ZnO/CdSe/CdTe/ZnTe:Cu	650	19.73	49.75	6.38	Yes

Because Sn and Pb doping in CdTe can cause compensation[100] effects and potential carrier lifetime reduction, it is suggested that research in this area proceed with caution—if sufficient group IV related recombination centers develop over time or with subsequent thermal processing, solar cell performance might be impacted. Group IV and Group V telluride back contact results are summarized in Table 4.

4.7 | Group V tellurides: arsenic, antimony, and bismuth tellurides

Tellurium does not form a stable compound with nitrogen, and phosphorus telluride bonds are weak.[101] Arsenic (III) telluride, antimony (III) telluride, and bismuth (III) telluride are all stable compounds. Nitrogen,[102] phosphorus,[103] arsenic,[104] and antimony[105] all dope CdTe p-type.

Sb_2Te_3 is a layered narrow-gap semiconductor with van der Waal's bonding between layers.[106] This forms an intermediate layer. The work function of Sb_2Te_3 is 5.8 eV, in theory a very good match to p-type CdTe. Sb excess is likely to dope CdTe p-type. Sb_2Te_3 contacts have been reported twenty years ago (Romeo et al (2000)[107]). Sb_2Te_3 contacts are reported to produce cells with PCE over 12% (Paudel et al (2011)[108]), when Cu is also used.

Arsenic telluride (As_2Te_3) is a narrow gap semiconductor with two crystal phases, monoclinic (most stable at ambient pressure) and rhombohedral. Although not as well studied as a back contact material for CdTe as is Sb_2Te_3, As_2Te_3 is likely to dope the interface region of the CdTe with arsenic. Al Turkestani (2007)[109] only obtained a PCE of 5.4% (V_{oc} 600 mV, J_{sc} 21.6 mA cm^{-2}, FF 41.5%), but this process had at the time a maximum 5.7% PCE with any

back contact technology (gold contact, no etch process). Al Turkestani's As_2Te_3 contacts outperformed his equivalent Sb_2Te_3 contacts (PCE 3.6%). Romeo et al (2010)[110] reported 15.8% PCE with As_2Te_3/Cu contacts—both deposited at 200°C, in this case outperforming Sb_2Te_3 contacts. Romeo et al (2017)[111] have had higher PCE, finding very similar results (15%-16%, FF 70%-72%) with As_2Te_3, Bi_2Te_3, and ZnTe and slightly reduced PCE with Sb_2Te_3. It is presumed that the toxicity of arsenic has sometimes driven the preferential choice of Sb_2Te_3 over As_2Te_3. When CdTe is heavily doped with arsenic, there is a possibility that some As_2Te_3 is formed at the rear surface.[104]

Bismuth telluride is a narrow gap semiconductor, with rhombohedral crystal symmetry, that can be doped n-type or p-type. Bismuth is a reasonably cheap and relatively non-toxic element. Lee and Myers (2015)[112] measured a valence band offset of 0.22 eV for the Bi_2Te_3/CdTe (111) interface. Romeo et al (2013)[113] used Bi_2Te_3 as a back contact material achieving 10.2% PCE (V_{oc} 775 mV, J_{sc} 22.9 mA cm^{-2}, and FF 57.5%). Tang et al (2014)[114] reported similar PCE and FF values, with a lower V_{oc}. Romeo et al (2017)[111] claim that there is little difference in performance between using Bi_2Te_3 and As_2Te_3. It would be interesting to see whether Bi_2Te_3 could be used on in situ p-type doped CdTe where any low-level n-type doping effect from Bi is unlikely to cause compensation.

5 | SELENIDE BACK CONTACTS

Selenides are often chemically like their sulfide counterparts. Many metals form stable selenides. Some of these have a two-dimensional layered structure. The only uses of binary

TABLE 4 Selected solar cell J-V parameters from CdTe solar cells with Group IV telluride (SnTe, PbTe) and Group V telluride (As_2Te_3, Sb_2Te_3, and Bi_2Te_3) back contacts reported in the literature

Reference	Contact	V_{oc} (mV)	J_{sc} (mA cm^{-2})	FF (%)	PCE (%)
Weng et al (2018)[95]	ZnTe/Cu/SnTe/metal	841	24.7	70.2	14.6
Shu et al (2019)[96]	SnTe/Ni	782	24.6	68	13.1
Swartz et al (2019)[99]	SnTe:Tl/Au	Unstated	Unstated	Unstated	13.5
Swartz et al (2019)[99]	PbTe:Tl	<700	Unstated	"Shunted"	9
Romeo et al (1999)[242]	Sb_2Te_3	858	23	74	14.6
Hodges (2009)[243]	Sb_2Te_3	820	21.3	70.0	12.2
Hu et al (2011)[244]	Sb_2Te_3	816	25.8	62.3	13.1
Emziane et al (2005)[245]	Sb_2Te_3/Mo	812	25	69	14
Paudel et al (2011)[108]	Sb_2Te_3/Cu/Au	778	22.1	71.8	12.3
Paudel et al (2011)[108]	Sb_2Te_3/Au	717	22.2	63.2	10.1
Al Turkestani (2007)[109]	As_2Te_3	~600	21.6	41.5	5.4
Romeo et al (2010)[110]	As_2Te_3/Cu	862	25.5	72	15.8
Romeo et al (2013)[113]	Bi_2Te_3	775	22.9	57.5	10.2
Tang et al (2014)[114]	Bi_2Te_3/Ni	650	26.9	60.7	10.6

metal selenides as back contacts to CdTe-based solar cells known to the authors are $TiSe_2$ and VSe_2. The promising work function value reported by Kraft et al (TSF 2003)[115] for VSe_2 did not produce Ohmic contacts when CdTe was deposited on these selenides. This was attributed to the formation of dipoles at the VSe_2 to CdTe interface with an excess of Cd present, due to a higher sticking coefficient of Cd.

Zhao (2008)[116] (University of South Florida) attempted to selenize titanium deposited on the back of a CdTe solar cell. However, the high temperatures required for selenization (>420°C) led to deterioration of the CdTe. Later, Ferekides and Morel (2011)[117] reported four candidate metal selenides: $TiSe_2$, VSe_2, $NbSe_2$, and $TaSe_2$ (no experimental work). Deposition of $TiSe_2$ onto CdTe by selenization of titanium required too high a processing temperature resulting in some CdTe sublimation.

Copper selenide would be a logical compound to try as a back contact, considering the other binary copper chalcogenides Cu_xTe and CuS reported. One reason for little work on these contacts might be that no good solar cell efficiencies have been achieved to date. The copper-selenium phase diagram is complex,[118] and several Cu-Se compounds exist.

No publications have been found on CdTe solar cells either with $NbSe_2$ or $TaSe_2$ contacts. However, attempts have been made to grow CdTe on $NbSe_2$ substrates.[119] Depositing $NbSe_2$ onto CdTe led to similar dipole formation issues as was reported for VSe_2 on CdTe. Gao et al (2014)[120] deposited VSe_2 by electron beam evaporation onto CdTe device structures with a copper-free process. The measured J-V curves had a high series resistance but did show an improvement over devices without the VSe_2 layer (with VSe_2 V_{oc} 716 mV, J_{sc} 20.65 mA cm^{-2} FF 60.5%, and PCE 8.95%).

A possible problem with some transition metal chalcogenide contacts is the existence, in many cases, of multiple phases, often of different stoichiometry. One example is titanium selenide, for which several compounds are reported: Ti_9Se_2,[121] $Ti_{11}Se_4$[122] and those listed in Murray (1986).[123] Studies of a set of a single-metal sulfide, metal selenide, and metal telluride counterparts would be interesting. In the case of selenides, any significant diffusion of Se into CdTe would lead to a reduction in bandgap which might change recombination rates at the rear interface. Selenide back contact solar cell results from the literature are summarized (along with sulfide back contacts) in Table 5. There are no reports of $MoSe_2$ back contacts known to the authors.

6 | SULFIDE BACK CONTACTS

The following metal sulfides are noted as having been used as CdTe back contact materials: CuS, $CuInS_2$, $CuInS_2$:N, CuS/ZnS, FeS_2, (Fe,Ni)S_2 and MoS_2. Other sulfur-containing materials are found listed under other categories (eg, BaCuSF under halides). Sulfide back contact solar cell results from the literature are summarized (with selenide back contacts) in Table 5.

Copper sulfide contacts were reported by Kim et al (2003).[124] The following J-V parameters were obtained: V_{oc} 840 mV, J_{sc} 19.5 mA cm^{-2}, FF 69.6%, and PCE 11.4%. The as-deposited films were not stoichiometric and required a thermal anneal at 200°C which changed the Cu/S ratio from ~0.75 to 0.95-1.05. Lei et al (2013)[125] obtained 12.2% (V_{oc} 820 mV, J_{sc} 21.6 mA cm^{-2}, and FF 68.9%) using a 75 nm thick CBD-grown Cu_xS film. Türck et al (2015)[126] obtained 13% PCE (V_{oc} "almost 800 mV," J_{sc} ~ 24 mA cm^{-2},

FF ~ 70%) after annealing at 225°C. Subedi et al (2017)[127] reported PCE 13% (V_{oc} 806 mV, J_{sc} 22.1 mA cm^{-2}, and FF 73%) using $(CuS)_x(ZnS)_{1-x}$/Cu/Au back contacts. With copper-containing back contacts, the effect of the back contact is difficult to separate from CdTe doping effects. Zakyutayev et al (2020)[128] used a $Cu_{0.60}Zn_{0.40}S$ back contact to achieve 13.8% PCE (V_{oc} 836 mV, J_{sc} 24.6 mA cm^{-2}, and FF 74.4%) using a process that gave 14.0% PCE with a ZnTe:Cu back contact.

Iron sulfide (iron pyrite, FeS_2) could be used as a potential back contact in a "Cu-free" process, but iron diffusion into CdTe must be considered. FeS_2 nanocrystals, deposited by drop-casting of nanocrystals in a chloroform solution, have been used (Bhandari et al (2015)),[129-132] as a back contact material. They also compared performance with and without the use of copper. With Cu, a PCE of 13.3% (V_{oc} 810 mV, J_{sc} 21.4 mA cm^{-2}, FF 72.8%, series resistance 3.1 Ω cm^2) was achieved. Without Cu, a PCE of 12.5% was achieved. As the energy gap of FeS_2 is only 0.95 eV, it will absorb light itself potentially increasing J_{sc}, because it is a p-type conductor (not forming an opposing diode). However, the conductivity is low so too thick a layer will add series resistance. $(Cu,Fe)S_2$, tried by Bastola et al (2018)[133] gave 12% PCE.

Nickel alloyed iron sulfide was used by Bastola et al (2017).[134] $Ni_xFe_{1-x}S_2$ was observed to be p-type with up to 10% Ni, but n-type for 20% or greater Ni content. As Ni content increased from 0% to 30%, V_{oc} increased monotonically from 834 to 848 mV, while J_{sc} decreased monotonically (rapidly above 20% Ni). FF reached a maximum at 5% Ni, as did efficiency (PCE 11.8%, V_{oc} 835 mV, J_{sc} 19.7 mA cm^{-2}, and FF 70.8%). The $Ni_{0.05}Fe_{0.95}S_2$/Au contact was a small (8% relative) improvement on their standard Cu/Au contact.

Nickel sulfide has been tried as a hole transport layer in perovskites[135] (Ni_xS composite with carbon gave low-performance perovskite solar cells with PCE ~ 5%, V_{oc} < 600 mV, FF < 40%), but no reports have been found using Ni_xS in CdTe solar cells.

Barium copper sulfide ($BaCu_4S_3$ or BCS) has been used by Subedi et al (2019)[136] in a recent bifacial solar cell study, in which ITO was deposited on top of ~100 nm of BCS on 3 μm of CdTe. Front-side (through glass) illumination gave PCE 12.3% (V_{oc} 823 mV, J_{sc} 21.2 mA cm^{-2}, FF 70.4%, and R_s 3.8 Ω cm^2), but only a PCE of 1% when rear illuminated (J_{sc} 2.8 mA cm^{-2}).

In the substrate configuration, X. Tan (2017)[137] at the University of Toledo has studied CIS and nitrogen-doped CIS as back contacts in glass/Mo/CIS/CdTe/CdS solar cells. The best PCE was only 3.84% in a variant structure (glass/Mo/MoO_X/CIS:N/CdTe/CdS).

Molybdenum sulfide (MoS_2) was used as a back contact material by Yuan et al (2017).[138] A study of different thicknesses of MoS_2 gave a maximum PCE of 13.7%. The estimated valence band offset between CdTe and MoS_2 was 0.56 eV, whereas Deng et al (2020)[139] estimated 0.46 eV. The

contact metal used by Yuan et al was gold (good work function match to MoS_2); nickel would have been an interesting comparison. It is noted that making Ohmic contacts to MoS_2 is itself not trivial.[140]

7 | METAL OXIDE BACK CONTACTS

Oxides are often used as transparent conducting front contact materials (eg, SnO_2:In (ITO), SnO_2:F (FTO), ZnO:Al (AZO)). Bandgap values are mostly larger than their sulfide, selenide, and telluride counterparts. As the properties of individual oxides vary considerably, it is better to discuss each oxide separately. However, an attempt is made to group 3d transition metal oxides, where there are some similarities such as the possibility of mixed valency of the metal in the case of molybdenum and vanadium oxides. Diffusion of 3d metal ions into CdTe must be considered, especially for those cases in which deep levels are formed which can in some cases dramatically decrease minority carrier lifetime.

The question of what role the oxygen plays at CdTe surfaces, interfaces, and grain boundaries is interesting. Air or oxygen anneals before metallization have been found to improve device performance in arsenic-doped CdTe[141] and some Cu-doped processes. Major (2016)[142] discussed the effect of oxygen on grain boundaries largely, but not completely, from the point of view of oxygen exposure during CdTe growth or the $CdCl_2$ activation process.

7.1 | Zinc oxide

Zinc (II) oxide (ZnO) is a wide-gap semiconductor with a wurtzite crystal structure and an ambient temperature bandgap of around 3.3 eV. ZnO heavily doped with aluminum (AZO) is a well-known transparent conducting oxide (TCO), and has been used both as a front contact,[143] and as a back contact material (Parikh (2007),[144] Heisler et al (2013)[145]) for CdTe absorber solar cells. Aluminum doping greatly increases the conductivity of ZnO and introduces a Moss-Burstein shift of the bandgap to higher photon energy.

Parikh,[144] using a thin 80 nm thickness of ZnO:Al obtained 1.79% PCE with no copper, and 5.74% PCE (V_{oc} 475 mV, J_{sc} 22.9 mA cm^{-2}, and FF 52.7%) with the use of copper before ZnO:Al deposition (and a short 150°C anneal). Heisler et al (2013)[145] used RF sputtered ZnO:Al back contacts with both 0.7 and 1.7 μm thick CdTe absorbers, obtaining a maximum PCE of 8.6% (best cell: V_{oc} 744 mV, J_{sc} 19.4 mA cm^{-2}, and FF 60%) for the thicker CdTe.

Duenow et al (2009)[146] published data on composite ZnTe:Cu/ZnO:Al back contacted CdTe cells (also ZnTe:Cu/

TABLE 5 J-V parameters of CdTe solar cells with selenide and sulfide materials as back contactS

Reference	back contact material	V_{oc} (mV)	J_{sc} (mA cm^{-2})	FF (%)	R_s (Ω cm^2)	PCE (%)
Gao et al (2014)[120]	VSe$_2$	716	20.65	60.5	131	8.95
Kim et al (2003)[124]	CuS	840	19.45	69.6	-	11.37
Türck et al (2015)[126]	Cu$_2$S	~800	~24	~70	-	13
Zhang et al (2016)[246]	Cu$_9$S$_5$	797	24.0	72.1	-	13.8
Lei et al (2013)[125]	Cu$_x$S/Ni	820	21.6	68.9	-	12.2
Bhandari et al (2015)[129]	FeS$_2$/Au (1 µm/30 nm) (no Cu)	811	23	67	-	12.5
Bhandari et al (2017)[130]	FeS$_2$ (with Cu)	810	21.4	72.8	3.1	13.3
Bastola et al (2017)[134]	(Fe$_{0.95}$Ni$_{0.05}$)S$_2$ (with Cu)	835	19.7	70.8	-	11.8
Rockett et al (2018)[247]	FeS$_2$/Au	811	23	68.9	~6	12.5
Rockett et al (2018)[247]	Cu/FeS$_2$/Au	803	22.5	70.9	-	12.8
Bastola et al (2018)[133]	Cu/CuFeS$_2$/Au	823	19.2	74.6	3.3	12
Yuan et al (2017)[138]	Cu/MoS$_2$/Au	752	25.9	70	-	13.7
Zakyutayev et al (2020)[128]	CuZnS	836	14.6	74.4	3.9	13.8

Note: Series resistance (R_s) is given when found within the reference.

ITO back contacts), obtaining 10.2% PCE (V_{oc} 798 mV, J_{sc} 20.7 mA cm^{-2}, and FF 61.7%).

7.2 | Indium oxides

Indium-doped tin oxide (ITO), a highly conductive n-type TCO, has been used as a back contact material. The use of ITO as a back contact interface material is not intuitive as ITO/CdTe junctions have been used as solar cells diode junctions.

Calnan (2008)[147] looked at the optical transmission of indium-doped metal oxides for front and back contacts to CdTe absorber cells,[148] but did not publish any CdTe absorber solar cell PCE data.

Romeo et. (2007)[149] obtained 10% PCE with a Cu/ITO back contact, i8nm a cell which was bifacial. Using nanocrystal CdTe in an ink, Crisp et al (2014)[150] obtained PCE 11.3% (V_{oc} 686 mV, J_{sc} 25.5 mA cm^{-2}, FF 64.7%) with a ZnO/CdTe/ITO device in which the n-p junction was between the ZnO and CdTe and ITO formed the back contact. Swartz et al (2019)[99] using an ITO/Au back contact on a CdTe nanoparticle treated CdTe absorber obtained PCE 14.7% with other J-V parameters not explicitly stated.

7.3 | Molybdenum oxide

Molybdenum (VI) oxide (MoO$_{3-x}$) is a wide bandgap semiconductor,[151] which when perfectly stoichiometric, has a layered structure. As oxygen is lost from MoO$_3$, the bandgap narrows, the material increases in conductivity, and the material structure becomes more complex. Metallic molybdenum (IV) oxide (MoO$_2$) can be formed from MoO$_3$ in reducing conditions.[152,153]

Table 6 lists several of the papers to publish results using MoO$_{3-x}$ as a back contact for CdTe absorber solar cells. Most of these results are on superstrate configuration cells, except where noted below. It can be seen from Table 6 that several different metals have been used on top of the MoO$_x$, this additional step adds a further complexity to the back contact and reduces the ability to directly compare results from the different groups. The top PCE reported for a MoO$_x$ back contact is 14.6% for a process which includes the use of copper[154] and 14.1% for a process which excludes copper.[155]

H. Lin (2012)[156] observed some Mo^{5+} formation when sputtering, but not when thermally evaporating molybdenum oxide. The minimum series resistance obtained was 4.7 Ω cm^2 with 40 nm of evaporated MoO$_{3-x}$ and nickel metallization. An advantage of the MoO$_{3-x}$ layer is that several low-cost metals (including aluminum) can be used on the MoO$_{3-x}$ surface; expensive, high work function metals are not necessary. However, the highest V_{oc} achieved by any researchers found in this analysis was using a gold metallization.[157] Lin et al[155] showed greater PCE stability of CdTe devices when using Ni or Mo metallization on MoO$_3$ at the back contact compared to the less stable Cr and Mg metals, and a very unstable Al contact. The stability tests used were a 19 hours anneal at 200°C and a 400 day light-soak.

Paudel and Yan (2014)[158] performed x-ray photoelectron spectroscopy measurements on the CdTe to MoO$_3$ interface finding a 2.75 ± 0.2 eV valence band offset (barrier to holes). Their FF decreased with increasing MoO$_3$ thickness from 2 nm

to 40 nm (series resistance increased). An increase in V_{oc} by 50 mV was observed when a 2 nm thick MoO_3 layer was used.

Gretener (2015),[153] using substrate configuration cells, concluded that MoO_2 was present at the CdTe interface in the highest performing cells. MoO_2 is expected to have a higher work function and more metallic conduction than MoO_3. Drayton (2015)[159] also found that low-temperature deposition MoO_x deposition gave MoO_2 XPS peak positions.

Ta_2O_5 has been successfully used as a high resistance layer between CdS and CdTe[160] (increasing V_{oc} and FF), but no results have been found using Ta_2O_5 as a back contact interfacial layer.

7.4 | 3d transition metal oxides

Vanadium oxide and nickel oxide have been used as CdTe absorber solar cell back contact materials. Transition metals from the 3d series often form deep levels within semiconductors. If CdTe carrier lifetime is reduced by the 3d transition metal, and there is a mechanism for diffusion, then that metal oxide is probably best avoided.

Vanadium can form the following oxides: V_2O_3, VO_2, and V_2O_5. The bandgaps of the vanadium (III) and vanadium (IV) oxides are narrow, only the vanadium (V) oxide bandgap is wide enough to be useful as a front contact, or as a back contact with high transmission in the visible or NIR. Deposited V_2O_5 films can have a range of bandgaps from 2.25 to 3.1 eV.

V_2O_5 is thermochromic that is its color (bandgap) changes rapidly (decreases) with increasing temperature.[161] Vanadium doping of CdTe can produce associated deep levels[162] and is used to produce very resistive CdTe.

Paudel et al (2015)[163] looked at three transition metal oxides (MoO_{3-x}, V_2O_{5-x}, and WO_{3-x}) with a view to making copper-free back contacts. Within these three systems, the best PCE was using molybdenum oxide (14.1% PCE, V_{oc} 815 mV, J_{sc} 25.4 mA cm^{-2}, FF 67.9%, and R_s 6.4 Ω cm^2), whereas the vanadium oxide cells gave 13.6% (V_{oc} 778 mV, J_{sc} 25.1 mA cm^{-2}, FF 69.4%, and R_s 6.2 Ω cm^2), and the tungsten oxide 12.9% (V_{oc} 767 mV, J_{sc} 24.6 mA cm^{-2}, FF 66.7%, and R_s 6.5 Ω cm^2).

Shen et al (2016)[164] obtained 10.4% PCE (V_{oc} 729 mV, J_{sc} 24.7 mA cm^{-2}, and FF 57.6%) using gold contacts to V_2O_5 back contacts. These results were further improved using a thin (2 nm) Cu layer before the V_2O_5 deposition leading to 13.7% PCE (V_{oc} 797 mV, J_{sc} 24.8 mA cm^{-2}, and FF 69.4%), very similar to Paudel el. (2015).[163] On timescales of up to a year, some PCE degradation was observed due to a small increase in series resistance.

Nickel (II) oxide (NiO), a p-type semiconductor, was used as a CdTe back contact by Ishikawa et al (2016)[165] and Xiao et al (2017).[166] Ishikawa et al used sputtered Ag-doped NiO back contacts. PCE with NiO:Ag was 5.14% (V_{oc} 598 mV, J_{sc} 16.4 mA cm^{-2}, and FF 53%), compared to a baseline carbon-based contact giving PCE 15.3%. In the work of Xiao et al PCE was maximized at 20 nm NiO thickness and further improved with a 3 nm thick layer of copper deposited before

TABLE 6 List of J-V characteristics from solar cells using molybdenum oxide in the back contact process, references and whether copper is used in the process

Reference	Device structure or contact	V_{oc} (mV)	J_{sc} (mA cm^{-2})	FF (%)	PCE (%)	Process contains copper
Yang et al (2016)[248]	CdTe/Cu/MoO$_x$/Cu-Au	799	25.3	70.1	14.2	Yes
Zhang et al (2018)[154]	CdTe/MoO$_x$/Cu	830	24.2	72.7	14.6	Yes
Wang et al (2018)[249]	CdTe/MoO$_3$/Mo	794	24.9	69.0	13.7	Yes
Hao Lin et al (2012)[155]	CdTe/MoO$_3$/Ni	808	22.0	72.6	12.9	No
Hao Lin et al (2012)[155]	CdTe/MoO$_3$/Al (superstrate)	815	22.3	68.4	12.4	No
Drayton et al (2015)[159]	Cu/MoO$_x$/Ni	792	21.9	68.3	11.9	Yes
Paudel et al (2015)[163]	MoO$_3$/Au	815	25.4	67.9	14.1	No
Paudel et al (2015)[163]	MoO$_3$/Au	790	22.6	65.0	11.6	No
Paudel et al (2013)[250]	Te/MoO$_3$/Cu	833	22.4	71.4	13.3	Yes
Perrenoud (2012)[152]	CdTe/MoO$_3$	329	16.4	38.5	2.1	No
Irfan et al (2012)[251]	MoO$_x$/Ni	807	20.7	70.8	11.8	Uncertain
Perrenoud (2012)[152]	Cu/Te/MoO$_x$	768	21.4	68.6	11.3	Yes
Gretener (2015)[153]	MoO$_x$/Te/CdTe (substrate)	733	22.0	62.3	10.0	Yes
Gretener (2015)[153]	MoO$_x$/CdTe	597	20.3	48.4	5.9	Yes
Dang and Singh (2015)[252]	Substrate/NW CdS/CdTe/ MoO$_{3-x}$/Au	752	25.6	57.1	11.0	No
Artegiani (2019)[157]	CdTe/MoO$_{3-x}$/Au	852	19.4	61.6	10.2	Yes

the NiO. Maximum PCE with the Cu layer was 13.5% (V_{oc} 791 mV, J_{sc} 23.7 mA cm^{-2}, FF 68.9%, and R_s 9.5 Ω cm^2); without Cu, the maximum PCE was 12.2% (rollover in forward bias). Degradation in PCE at 80°C was reduced with 20 nm NiO in the back contact.

Alloying nickel oxide with cobalt[167] (Ni$_{1-x}$Co$_x$O$_2$) is a possibility for fine tuning of the material's electron affinity (probably at the expense of conductivity).

Titanium dioxide (TiO$_2$) is widely used as an electrode material in organic solar cells. However, it has not been tried (to the authors' knowledge) as a CdTe solar cell back contact material probably due to its expected high valence band offset (2.6 eV[168]). TiO$_2$ has been used as an n-type buffer layer[169] for p-CdTe absorber solar cells. Titanium metal has been used as a back contact (NREL 2009).[146] Oxide formation over time could lead to a possible TiO$_2$ intermediate layer. Long-term diffusion of Ti into CdTe might reduce doping levels due to deep level formation.[170]

No other 3d transition metal oxides are known to have been used as CdTe absorber solar cell back contact materials.

7.5 | Aluminum oxide

Very thin layers of aluminum oxide (Al$_2$O$_3$) have been suggested as passivation layers for the rear surface of CdTe. Al$_2$O$_3$ has a very large bandgap and is typically very insulating. An Al$_2$O$_3$ barrier must be very thin to enable electrons to tunnel through. For very thin layers, there is the issue of uniformity, do areas exist with missing Al$_2$O$_3$ or thicker regions exist where tunneling is inhibited? This is a difficult characterization issue at a buried interface that is also typically very rough.

The motivation for this approach is that minority carrier lifetimes have been observed to increase in some semiconductor systems when Al$_2$O$_3$ is applied to the surface (eg, HgCdTe,[171] Si,[172] and CIGS[173]). However, in a solar cell, the interface must pass current and impressive increases in lifetime in Al$_2$O$_3$ passivated CdTe[174] have not been developed into cells with excellent PCE.

There is also the question of whether copper is used in the process, so the interface in some studies can be to other materials (eg, CdTe/Cu$_x$Te/Al$_2$O$_3$[175]), rather than directly depositing Al$_2$O$_3$ onto CdTe.

Atomic layer deposited (ALD) Al$_2$O$_3$ on TEC™ 10 substrates has also been used to overcome shorts due to pinholes in CdTe solar cells (TEC™ 10/Al$_2$O$_3$/CdS/CdTe/ZnTe:Cu/Ni).[176] Liang et al (2015)[177] obtained PCE 12.1% using 1 nm thick ALD Al$_2$O$_3$. Lin et al (2016)[178] achieved PCE of 13.0% (V_{oc} 782 mV, J_{sc} 24.2 mA cm^{-2}, and FF 68%) with a 9 nm Cu back contact layer followed by a 2 nm ALD-Al$_2$O$_3$ layer. Munshi et al (2018)[179] achieved PCE 16.5% (V_{oc} 827 mV, J_{sc} 28.1 mA cm^{-2}, and FF 71.1%) with a thin 0.5 nm Al$_2$O$_3$ layer, but this was with dual Cd(Se,Te)/CdTe absorber layers which gave slightly higher V_{oc} and FF (same J_{sc}) without the Al$_2$O$_3$ layer.

7.6 | Copper oxide

There are three stoichiometric copper oxide compounds (Cu$_2$O, CuO, and Cu$_3$O$_4$).[180] Copper (I) oxide (Cu$_2$O) is a p-type semiconductor with a bandgap of ~2.1 eV. The contact resistance of Cu$_x$O on p-type CdTe was measured by Ghosh et al (2002).[181] The contact resistance measurement of 2.2×10^{-2} Ω cm^2 appeared favorable compared to similar measurements the authors performed on Ni-P/Au, Cu/Au, or Sb/Au contacts. Türck et al (2016)[182] obtained PCE 15.2% (V_{oc} 832 mV, J_{sc} 25.0 mA cm^{-2}, and FF 73.1%) on a CdTe absorber cell on TEC™ 15M substrate with CdS:O buffer and a Cu$_2$O/Au back contact. Heat treatment was required after Cu$_2$O deposition to achieve high PCE. Masood et al (2017)[183] at the University of Science and Technology of China, Hefei estimated the barrier height at the CuO/CdTe interface to be around 0.35-0.44 eV. Their best PCE was 12.2% (V_{oc} 753mV, J_{sc} 26.7 mA cm^{-2}, and FF 60.2%) with 10 nm CuO deposited before gold metallization. Cu$_2$O has also been used as a HTM in perovskite solar cells,[184] and its electronic properties compared with other copper compounds.[15]

7.7 | Oxide back contacts compared

Table 7 shows a comparison of the highest PCE CdTe absorber solar cells found in the literature using different oxide back contact materials. The maximum V_{oc} with an oxide back contact is about 830 mV—this is 20-40 mV below the maximum V_{oc} routinely achieved in several laboratories in recent years. J_{sc} is more difficult to compare between different laboratories, but with five reports of oxide materials greater than 24 mA cm^{-2} some oxides can certainly pass significant current at zero bias. No FF above 73.1% has been achieved with an oxide back contact.

It would be interesting to see more oxide materials applied to graded Cd(Se,Te) absorber solar cells.

8 | METAL PNICTIDE BACK CONTACTS

Metal pnictides have been little used as back contacts. Two examples of CdTe back contacts using single-metal nitrides have been found: ZrN (PCE 1.68% in 2014[185]) and MoN$_x$ (Guntur (2011[186]), Drayton et al (2015)[159] (PCE 5.24%). A more recent article (Kindvall et al (2017)[187]) on the use of MoN$_x$ (and MoO$_x$) on substrate configuration cells did not

TABLE 7 Comparison of best CdTe absorber solar cell performance with different oxide back contactS

Reference	Oxide back contact	V_{oc} of maximum PCE cell (mV)	J_{sc} of maximum PCE cell (mA cm^{-2})	FF of maximum PCE cell (%)	PCE (%)
Türck et al (2016)[182]	Cu$_2$O	832	25.0	73.1	15.2
Zhang et al (2018)[154]	CdTe/MoO$_x$/Cu	830	24.2	82.7	14.6
Shen et al (2016)[164]	V$_2$O$_5$	806	24.8	70.0	14.0
Paudel et al (2013)[250]	WO$_{3-x}$	787	24.6	66.7	12.9
Xiao et al (2017)[166]	Cu/NiO	796	24.2	70.2	13.5
Heisler et al (2013)[145]	ZnO:Al	745	19.3	64	9.3
Khrypunov et al (2019)[253]	ITO	808	18.7	69	10.4
Swartz et al (2019)[99]	ITO/Au	-	-	-	14.7
Wu et al (2006)[254]	Cu$_x$Te/ITO	806	25.0	69.2	13.7

explicitly state PCE values but did contain numerous J-V parameters presented in graphic form. When a thick MoN$_x$ film was used as a back contact, the J-V curves appeared very similar (PCE 12.3%, V_{oc} ~ 780-800 mV, J_{sc} ~ 23 mA cm^{-2}, FF ~ 70%, estimated from graphs) to their control device (Te then Ni based paint).

ZrN has been used as a CIGS back contact[188]—optically reflective but with increased series resistance and interface recombination. MoN has been used as a diffusion barrier in CIGS solar cells.[189]

Nickel phosphide was considered as a back contact material.[190] In this case, Ni$_2$P powder was mixed with the graphite paste applied to the back contact.

The use of pnictides within CdTe absorber solar cell back contact structures is not particularly mature, and no advantage over more established back contact technologies has yet been achieved.

9 | INORGANIC BACK CONTACTS CONTAINING HALIDES

Some complex fluorides have been suggested as p-type transparent contact materials.[191] Spies (2007)[192] at Oregon State University examined the use of barium copper tellurium fluoride (BCTF, bandgap 2.3 eV, hole concentration of 10^{20}-10^{21} cm^{-3}, mobility 1-5 cm^2 V^{-1} s^{-1}) as a CdTe absorber solar cell back contact. A PCE of 1.2% was obtained (V_{oc} 540 mV, J_{sc} 4.8 mA cm^{-2}, and FF 46%).

A collaboration in Japan between Ryukoku University and the Kisarazu National College of Technology, Chiba, has studied PLD quaternary chalcogenide fluoride materials for back contacts. Their first paper (2014) used the selenide-fluoride BaCuSeF.[193] A PCE of 2.82% (V_{oc} 796 mV, J_{sc} 6.0 mA cm^{-2}, and FF 59%) was obtained, which increased to 3.18% (V_{oc} 714 mV, J_{sc} 9.21 mA cm^{-2}, and FF 41%) with the inclusion of a thin Ni$_{0.97}$Li$_{0.03}$O interlayer. PCE was improved with a bromine-based back-surface treatment[194] (PCE

9.91%, V_{oc} 805 mV, J_{sc} 22.1 mA cm^{-2}, and FF 55.7%). It is noted that a Cu$_x$Te layer formed during processing with x ~ 1.4. Using strontium instead of barium and improving back-surface conductance by using ITO on top of the fluoride layer[195] improved the PCE to 14.3% (V_{oc} 804 mV, J_{sc} 27.5 mA cm^{-2}—very high if reproducible, FF 65%). The optimum thickness of SrCuSeF was 34 nm (with 200 nm of ITO on top). The authors believe that the low conductivity of the fluoride layer is limiting series resistance and hence FF. Doping with sodium[196] gave a small improvement in FF raising the PCE to 14.7% (V_{oc} 806 mV, J_{sc} 27.5 mA cm^{-2}, and FF 66.1%). Substituting sulfur for selenium (BaCuSF),[197] again used with ITO on top (platinum metallization), gave PCE 13.9% (V_{oc} 818 mV, J_{sc} 25.2 mA cm^{-2}, and FF 67.5%).

The use of quaternary inorganic materials allows a huge range of potential materials to be considered. However, controlling the composition of many quaternary materials can often be difficult compared to ternary or binary materials, as well as allowing a large range of potential native defects.

Perovskite halide back contacts to CdTe devices have been studied by the University of Toledo group.[198,199] Small performance gains (4-9 mV in V_{oc}, 1.4%-2.1% in absolute FF) were achieved over their standard Cu/Au back contacts. Some devices gave V_{oc} 870 mV which the authors said they would investigate further. The authors also have used the reaction of methylammonium iodide (MAI) with cadmium (forming (CH$_3$NH$_3$)$_2$CdI$_4$ (or MA$_2$CdI$_4$) perovskite in solution) to selectively remove Cd from the back surface, leaving the surface Te-rich. Either copper/gold or ITO contacts (transparent) were then applied. MAI treated CdTe with Cu/Au (0.5 nm Cu) contacts achieved 13.0% average PCE (V_{oc} 824 mV, J_{sc} 20.5 mA cm^{-2}, and FF 77.1%) and 13.5% in the champion cell. MAI treated CdTe with Cu/ITO back contacts achieved PCE 12.2% (V_{oc} 823 mV, J_{sc} 21.4 mA cm^{-2}, and FF 69.3%); MAI treated CdTe with Cu-free ITO back contacts gave a champion cell with PCE 10.0% (V_{oc} 748 mV, J_{sc} 21.0 mA cm^{-2}, and FF 57.9%). The Cu-free cell therefore had reduced V_{oc} and FF.

Copper (I) iodide has been used as a back contact material (Li et al (2019)[200]). PCE was maximized with a very thin (5 nm) CuI layer (PCE 14.5%, V_{oc} 795 mV, J_{sc} 25.4 mA cm^{-2}, FF 71.9%, and R_s 3.6 Ω cm^2). CuI has also been used as a perovskite HTM.[15] Copper (II) chloride has been used by Artegiani et al (2019).[201] In this case, the copper halide is thought to be acting as a reproducible source for a very small amount of copper (equivalent to 0.1 nm of pure copper) leading to an improvement in device stability after 1000 hours of 80°C stress testing.

Copper is common to all the halide-based back contact technologies listed in Table 8; of the back contact materials in Table 8, only perovskites are potentially compatible with a Cu-free process.

10 | INORGANIC CARBON-BASED BACK CONTACTS

In this section, carbon allotrope back contacts and some materials containing carbon atoms are examined. Several forms of carbon have been used as back contacts, perhaps reflecting the wider research of the time on an allotrope. Graphite is a low-cost material which can be formed easily into a cheap paste, which is often convenient for small laboratories. Such pastes can also be loaded with metal particles, such as copper or silver, or as mentioned earlier HgTe.

The use of graphene with thin film solar cells including CdTe has been reviewed recently (Shi and Jayatissa (2018)[202]); this included the usage of graphene in the front contact. Cu nanowires combined with graphene were used by Liang et al (2012)[203] (PCE 12.1%, V_{oc} 801 mV, J_{sc} 22.4 mA cm^{-2}, and FF 67.4%); this could be just a reasonably effective way of delivering restricted amounts of copper to the back surface. Graphene has been studied, doped with boron by Lin et al (2011)[204] (PCE 7.86%, V_{oc} 674 mV, J_{sc} 22.0 mA cm^{-2}, and FF 55.2%).

Single-Walled carbon nanotubes (SWCNT) have also been used. Barnes et al (2007)[205] used SWCNTs as a transparent back contact on top of Cu$_x$Te on CdTe (PCE 12.4%). Khanal's Cu-free SWCNT device[206] reached 11.3% PCE (V_{oc} 788 mV, J_{sc} 21.8 mA cm^{-2}, and FF 66.5%). Phillips et al (2013)[22] reported further work on SWCNT/Au contacts, reporting 11.0 ± 2.8% PCE. Bin Li et al (2016)[207] obtained 9.71% PCE (V_{oc} 692 mV, J_{sc} 22.7 mA cm^{-2}, and FF 61.9%) after a 320°C annealing step. Alfadhili et al (2017)[208] attempted to dope SWCNTs with triethyloxonium hexachlorantimonate increasing V_{oc} but adversely impacting FF (best results: PCE 10.6%, V_{oc} 805 mV, J_{sc} 19.4 mA cm^{-2}, and FF 68.9%).

The mobility of individual nanotubes is very high, up to 10^5 cm^2 V^{-1} s^{-1}, but the effective sheet resistance remains high compared to good TCOs, at over 500 Ω/sq at a film thickness of 500 nm, due to relatively poor conduction between nanotubes. This is a generic issue with nanowire structures in any material

for use as a carrier transport layer in solar cells: both internal conductivity and effective contact conductance need to be high.

Koirala et al (2014)[209] studied PECVD grown silicon alloyed with carbon, heavily p-type doped with hydrogen and boron (a-Si$_{1-x}$C$_x$:H) as a CdTe back contact material. The devices had a high series resistance (12 Ω cm^2), reducing FF (48.8%) compared to their reference Cu/Au contacts (FF 67%).

Considering carbon containing compounds, Paudel and Yan (2016)[210] tried copper thiocyanate (CuSCN) back contacts. This was not the first use of CuSCN as a back contact as Tena-Zaera et al (2005)[211] had used it in a thin absorber solar cell of structure ZnO/CdTe/CuSCN, obtaining very poor preliminary solar cell J-V parameters (V_{oc} ~ 200 mV, J_{sc} < 1 mA cm^{-2}, and FF 28%). A high PCE of 13.7% was obtained (V_{oc} 866 mV, J_{sc} 22.9 mA cm^{-2}, and FF 69.1%, R_s 6.6 Ω cm^2) with a 5 nm thick CuSCN layer. CuSCN, a wide bandgap (3.4-3.9 eV) p-type semiconductor,[212] has been used successfully as a HTM with perovskites, reportedly improving their thermal stability compared to many organic HTMs,[213] and acting as a passivation agent for unbonded lead. Similar CdTe solar cell PCE values were obtained by Pressman (2017)[214] at the University of Liverpool (PCE 13%, V_{oc} 780 mV, and J_{sc} 26 mA cm^{-2}). Montgomery et al (2019)[215] (University of Alabama) used two different solvents to deposit CuSCN on the back of a CdSe-CdTe solar cell obtaining 17% PCE, using a CdSe buffer the results are not entirely comparable to CdS buffer cells, but the V_{oc} and FF are very good. Forward-bias rollover is suppressed with CuSCN contacts. It is difficult to deconvolve the thiocyanate intermediate layer from copper doping effects. AgSCN has also been used by the Alabama group (Yan et al (2019)[216]).

Selected experimental solar cell parameter results from the literature for carbon containing inorganic contacts are collected in Table 9.

11 | ORGANIC MATERIALS AS BACK CONTACTS

Organic contacts can provide interlayers on CdTe. Several materials have been tried, mostly HTMs that have been commonly used before in polymer, DSSC, and perovskite solar cells. Thermal stability is important—the melting point and glass transition temperature must be sufficiently high that solar cell fabrication can be completed, and the finalized cell is stable in use. Most of the work in this area is in its infancy, despite work in the late 1990s on the surface chemistry of organic molecules on CdTe (Cohen et al (1998)[217,218]).

An early reference found to J-V results on an organic back contact for p-type CdTe solar cells is by Jarkov (2011)[219] (Tallinn University of Technology). This study used PEDOT:PSS (poly(3,4-ethylenedioxythiophene): poly(-styrenesulfonate)) with conductivity enhancing additives, which gave a (Cu-free process) PCE of 3.8% (V_{oc} 610 mV,

TABLE 8 J-V parameters for CdTe absorber solar cells with halide and chalcogenide-halide back contact materials taken from the literature

Reference	Material	V_{oc} (mV)	J_{sc} (mA cm^{-2})	FF (%)	PCE (%)
Yanagi et al (2007)[191]	BaCuTeF	540	4.8	46	1.2
Yamamoto et al (2015)[194]	BaCuSeF	805	22.1	55.7	9.9
Miki et al (2018)[197]	BaCuSF/ITO	818	25.2	67.5	13.9
Kitabayashi et al (2017)[195]	SrCuSeF/ITO	804	27.5	65	14.3
Wada et al (2018)[196]	SrCuSeF:Na/ITO	806	27.5	66.1	14.7
Bhandari et al (2017)[198]	Cu/MAPb(Br$_{0.1}$,I$_{0.9}$)$_3$/Au	838	19.6	77.2	12.7
Bhandari et al (2017)[198]	Cu/MAPb(Br$_{0.3}$,I$_{0.7}$)$_3$/Au	836	20.2	77.5	13.1
Bhandari et al (2017)[198]	Cu/MAPb(Br$_{0.5}$,I$_{0.5}$)$_3$/Au	839	19.3	77.8	12.6
Bhandari et al (2017)[198]	Cu/MAPb(Br$_{0.7}$,I$_{0.3}$)$_3$/Au	841	20.0	77.1	13.0
X. Li et al (2019)[200]	CuI	795	25.4	71.9	14.5

J_{sc} 17.8 mA cm^{-2}, and FF 36%). However, the highest PCE of the reference process was only 6.6%. Later Wang et al (2016)[220] obtained 5.5% (V_{oc} 640 mV, J_{sc} 19.1 mA cm^{-2}, and FF 48%) with the most highly doped of their samples. Bromine-methanol etching before PEDOT:PSS deposition further improved performance to PCE 9.1% (V_{oc} 710 mV, J_{sc} 21.4 mA cm^{-2}, and FF 60%).

Jarkov et al (2013)[221] later tried electrodepositing polypyrrole-based back contacts: obtaining 10.4% PCE for polypyrrole doped with ß-naphthalene sulfonate (V_{oc} 739 mV, J_{sc} 20.9 mA cm^{-2}, and FF 67.1%). Earlier work by Koll et al (2011)[222] at the University of Toledo had shown pyrrole surface treatments to leave the surface Te-rich, as well as having a possible pinhole filling role.

Ferekides and Morel (2011)[117] published a summary report of a contract which looked at many back contact technologies, including the effect of several polymer materials used as back-interface materials with Mo metal contacts. The justification for their use was given in terms of surface dipole modification of the metal work function. The summary report gives little detail on materials, methods, or results, and the polymer work was stated to be "for all practical purposes very preliminary." Polymers derived from the monomers 4-methoxybenzoic acid (p-anisic acid), 4-chlorobenzoic acid, and 4-cyanobenzoic acid were spin-coated onto CdCl$_2$ treated CdTe, before Mo contact deposition. Some increase in V_{oc} was observed but the device technology was not optimized to minimize series resistance. No results for these polymers are included in the organic back contacts summary given in Table 10.

Spiro-OMeTAD (N2,N2,N2′,N2′,N7,N7,N7′,N7′-octakis (4-methoxyphenyl)-9,9′-spirobi[9H-fluorene]-2,2′,7,7′-tetramine) is another common HTM used in DSSC and perovskite solar cells. Spiro-OMeTAD hole mobility is very low (~10^{-5}-10^{-3} cm^2 V^{-1} s^{-1}[223]), so a higher conductivity material is required on top. Spiro-OMeTAD is commonly doped and oxidized to increase conductivity. A very common dopant contains lithium,[224] which could diffuse into the CdTe and affect the cell stability. Du et al (2015)[225] saw an improvement in nanocrystal CdTe solar cells when using spiro-OMeTAD as a replacement HTM for MoO$_{3-x}$. Shalvey et al (2018)[226] saw that Li-doped spiro-OMeTAD reduced forward-bias rollover in CdTe solar cells, but increased ambient temperature series resistance, resulting in no increase in PCE. Research on improving spiro-OMeTAD and similar materials intended as perovskite HTMs could also possibly benefit CdTe solar cells.

P3HT (Poly(3-hexylthiophene-2,5-diyl)) was found by Major et al (2017)[227] to act as a pinhole blocker and a back contact material. Shunt resistance was significantly improved, giving better yield and reduced FF spread. P3HT/CdTe interface has also been examined in CdTe quantum dots.[228] Abdul-Manaf et al (2014)[229] used polyaniline as a pinhole blocking layer. Separating out pinhole blocking and back contact interface effects is not trivial, and no study to date has given a comprehensive treatment of this issue.

Doped P3HT, with a similar HOMO level to spiro-OMeTAD, gave similar results[226] to spiro-OMeTAD. However, Shalvey et al (2018),[226] also tried PFO (Poly(9,9-di-n-octylfluorenyl-2,7-diyl)), which has a much deeper HOMO level, and found a reduced PCE (9.8%), with enhanced forward-bias rollover.

Another way of viewing the use of an organic intermediate layer between the CdTe and the metal back contact is as a method of modifying the metalwork function (de Boer et al (2005)[230]). Exact metal work functions often depend on crystal face.

Cobalt phthalocyanine (CoPC) contacts were used by Paudel and Yan (2014)[231] achieving 14.3% PCE (V_{oc} 815 mV, J_{sc} 24.2 mA cm^{-2}, FF 72.3%, and R_s 2.7 Ω cm^2) in a device free of forward-bias rollover. Maximum V_{oc} was found to be for a 10 nm thick CoPC layer. Copper phthalocyanine (CuPc) has been used as a HTM in perovskites (eg, Ke et al (2015)[232] PCE 14.7%) but only in 2019 (Varadharajaperumal et al (2019)[233]) was it used as a CdTe solar cell back contact. In a process with a low 1.3% baseline efficiency, a PCE of 2.7% was achieved.

TABLE 9 Selected CdTe absorber solar cell results from the literature using carbon containing inorganic back contacts (including carbon allotropes, carbides and thiocyanates)

Reference	Back contact or device structure	V_{oc} (mV)	J_{sc} (mA cm^{-2})	FF (%)	PCE (%)
Liang et al (2012)[203]	Cu NW/graphene	801	22.4	67.4	12.1
Lin et al (2011)[204]	B-doped graphene	674	22.0	55.2	7.86
Alfadhili et al (2017)[208]	Doped SWCNT	805	19.4	68.9	10.6
Phillips et al (2013)[22]	SWCNT	773	21.2	67.2	11.0
Khanal (2014)[206]	SWCNT	779	21.8	66.5	11.3
Koirala et al (2014)[209]	a-Si$_{1-x}$C$_x$:H	713	22.1	48.8	7.7
B. Li et al (2016)[207]	SWCNT/Au	692	22.7	61.9	9.7
Paudel & Yan (2016)[210]	CdTe/CuSCN/Au	866	22.9	69.1	13.7
Pressman (2017)[214]	CuSCN	780	26	~64	13
Montgomery et al (2019)[215]	CdSe/CdTe/CuSCN	860	28.2	70.3	17.0

The performance potential of metal phthalocyanines as back contacts in CdTe has not been fully explored.

Phenyl-C61-butyric acid methyl ester (PCBM), which contains a fullerene group, was used by Walkons et al (2014)[234] as a CdTe back contact layer and gave a low maximum PCE of ~3% (V_{oc}, J_{sc}, and FF were all poor); a back contact barrier height of 0.6 V was estimated from series resistance vs temperature measurements.

Pentacene was investigated by Perrenoud (2012)[152]—a PCE of 8.8% was obtained with no etching and no copper applied (low J_{sc} is possibly due to poor quality glass/TCO used in this experiment). Undoped pentacene is a p-type semiconductor; derivatives can have high hole mobilities for organic materials (>1 cm^2 V^{-1} s^{-1}).

Swartz et al (2019),[99] in a set of experiments using CdTe nanoparticles as cavity fillers in CSS-grown CdTe absorber devices, tried another proven perovskite hole contact material, spin-coated EH44 (2,7-Di(N,N-dimethoxyphenylamino)-N-(2-ethylhexyl)carbazole), as an interlayer between CdTe and a gold metallization achieving PCE 15%. EH44 is believed to have a glass transition temperature of only 69°C (lower than spiro-OMeTAD) but unencapsulated perovskite stability at 50°C was improved with EH44 compared to spiro-OMeTAD).

Table 10 shows CdTe solar cell performance results with organic materials as back contacts. V_{oc} values above 700 mV are achieved with all materials, raising V_{oc} above 800 mV appears more challenging with organic back contacts. J_{sc} values are often good, vertical transport of carriers through very thin organic layers is good enough. Achieving FF above 70% appears difficult: low mobility values require very thin layers to avoid significant increases in series resistance.

It is beyond the scope of this review to examine the valence band offsets to CdTe for every material in this review.

12 | SUMMARY

The search for an ideal back contact for p-type CdTe solar cells has not yet found a single solution. While back contact quality is not the only limiting factor in CdTe absorber solar cell performance, choosing poor contact materials can limit photovoltaic conversion efficiency or lead to degradation over time.

If the highest efficiency is required, a metallic or near metallic conductivity is necessary. At the same time, the interface must have a low defect density to avoid excessive carrier recombination. An ideal back contact will act as an electron reflector. Carriers need to arrive at the rear contact, so high carrier lifetime within the CdTe is a precondition, as well as a low density of defects at grain boundaries and the rear interface.

Similarities between the CdTe back contact issue and the hole transport layer in perovskite solar cells are noted. The range of organic materials used as HTMs in the extensive but less mature perovskite solar cell literature is already large. Concerns common to CdTe and perovskite solar cells include the thermal stability of the contact material itself, encapsulation, maximizing transport layer conductance, dopant diffusion, and cost of materials. Wide-gap perovskites are often aimed at tandem cell architectures and therefore require high NIR transparency. The following nonexclusive list of inorganic materials has been used as back contacts for both CdTe and perovskite solar cells: MoO_x, NiO, CuO_x, MoS_2, V_2O_5, NiS, CuSCN, CuI, CuPc, and carbon allotropes. Organic HTMs used on perovskite materials are too numerous to mention here and have been reviewed recently by Urieta et al (2018)[235] and Pitchaiya et al (2020).[15] A small fraction of these organic materials already has been used as CdTe back contacts—a systematic approach to their trial would be useful considering not

TABLE 10 J-V results from articles reporting organic materials as back contacts to CdTe absorber solar cells

Reference/comments	Organic back contact or interface layer	V_{oc} (mV)	J_{sc} (mA cm^{-2})	FF (%)	PCE (%)	R_s (Ω cm^2)
Swartz et al (2019)[99]	EH44/Au	-	-	-	15	
Paudel and Yan (2014)[231]	13 nm CoPc/Au	815	24.3	72.3	14.3	4.9
Major et al (2017)[227]	P3HT [no Cu]	841	25.5	66.5	14.25	
Major et al (2017)[227]	P3HT [with Cu]	767	22.8	65.7	11.54	
Walkons et al (2014)[234]	P3HT	780	22.3	70.8	12.26	
Wang et al (2016)[220]	PCBM/Pt	700-800	21 (at best, estimated)	low	~3	~100
Jarkov et al (2011)[219]	PEDOT:PSS	610	17.8	36.0	3.8	-
Wang et al (2016)[220]	PEDOT:PSS	710	21.4	60	9.1	
Jarkov et al (2013)[221]	PEDOT:PSS/C/Ni	795	22	72.3 (est.)	12.65	
Perrenoud (2012)[152]	Pentacene/Au	753	18.1	64.6	8.8	
Jarkov et al (2013)[221]	Polypyrrole	757	27.1	54.0	11.25	-
Shalvey et al (2018)[226]	Spiro-OMeTAD	750	22.7	59.4	11.26	
Shalvey et al (2018)[226]	PFO	750	25.3	50	9.81	

only band alignment but also their long-term stability and compatibility with a metal or other very high conductivity material. The only inorganic perovskite HTMs mentioned by Pitchaiya et al not known to have been used on CdTe are $CuCrO_2$ and $CuGaO_2$.

The ability to dope p-type CdTe using group V elements up to and above the 10^{16} cm^{-3} level allows the back contact to be decoupled from the requirement for including copper-containing compounds in the back contact structure: A wider choice of materials is available.

Ultimately, material costs matter, and any expensive materials removed from a process. In terms of impure elements, tellurium cost is expected to be the largest single component of the materials bill of thin film CdTe solar cells. Expensive metals such as gold or platinum are useful in fundamental studies but too costly in production. As tellurium is a moderately rare element itself, a crude guide is that any material used in the CdTe cell should cost significantly less than Te.

Promising materials include thin interlayers of stable materials that will not diffuse out to dope CdTe. Organic layers offer the widest range of tuneablity but need to be engineered to be stable at subsequent processing temperatures. Other suggestions for further trial include Bi_2Te_3 on arsenic-doped CdTe; MoS_2/Ni, copper-free thiocyanates and phthalocyanines, and a wider selection of perovskite like halides than has been tried until now.

ORCID
Ralph Stephen Hall https://orcid.org/0000-0002-7579-6838
Dan Lamb https://orcid.org/0000-0002-4762-4641
Stuart James Curzon Irvine https://orcid.org/0000-0002-1652-4496

REFERENCES
1. Shockley W, Queisser HJ. Detailed balance limit of efficiency of P-n junction solar cells. *J Appl Phys*. 1961;32(3):510-519. https://doi.org/10.1063/1.1736034
2. *Best Research-Cell Efficiency Chart*. https://www.nrel.gov/pv/cell-efficiency.html. Accessed Nov 14, 2019
3. Britt J, Ferekides C. Thin-film CdS/CdTe solar cell with 15.8% efficiency. *Appl Phys Lett*. 1993;62(22):2851-2852. https://doi.org/10.1063/1.109629
4. *First Solar Achieves Yet another Cell Conversion Efficiency World Record*. https://investor.firstsolar.com/news/press-release-details/2016/First-Solar-Achieves-Yet-Another-Cell-Conversion-Efficiency-World-Record/default.aspx. Accessed Nov 14, 2019
5. Green MA, Dunlop ED, Levi DH, Hohl-Ebinger J, Yoshita M, Ho-Baillie AWY. Solar cell efficiency tables (version 54). *Prog Photovolt Res Appl*. 2019;27(7):565-575. https://doi.org/10.1002/pip.3171
6. *First Solar Series 6 Module*. http://www.firstsolar.com/en-EMEA/Modules/Series-6. Accessed Nov 14, 2019
7. Wei S-H, Zhang SB, Zunger A. First-principles calculation of band offsets, optical bowings, and defects in CdS, CdSe, CdTe, and their alloys. *J Appl Phys*. 2000;87(3):1304-1311. https://doi.org/10.1063/1.372014

8. Ponpon JP, Siffert P. Barrier heights on cadmium telluride Schottky solar cells. *Rev Phys Appl (Paris)*. 1977;12(2):427-430. https://doi.org/10.1051/rphysap:01977001202042700

9. Wald FV. Applications of CdTe. A review. *Rev Phys Appl (Paris)*. 1977;12(2):277-290. https://doi.org/10.1051/rphysap:01977001202027700

10. Fahrenbruch AL. Ohmic contacts and doping of CdTe. *Solar Cells*. 1987;21(1–4):399-412. https://doi.org/10.1016/0379-6787(87)90138-4

11. Demtsu SH, Sites JR. Effect of back-contact barrier on thin-film CdTe solar cells. *Thin Solid Films*. 2006;510(1–2):320-324. https://doi.org/10.1016/j.tsf.2006.01.004

12. Williams RH, Patterson MH. Fermi level pinning at metal-CdTe interfaces. *Appl Phys Lett*. 1982;40(6):484-486. https://doi.org/10.1063/1.93151

13. Platzer-Björkman C, Barreau N, Bär M, et al. Back and front contacts in Kesterite solar cells: state-of-the-art and open questions. *J Phys Energy*. 2019;1(4):044005. https://doi.org/10.1088/2515-7655/ab3708

14. Karade V, Lokhande A, Babar P, et al. Insights into Kesterite's back contact interface: a status review. *Sol Energy Mater Sol Cells*. 2019;200:109911. https://doi.org/10.1016/j.solmat.2019.04.033

15. Pitchaiya S, Natarajan M, Santhanam A, et al. A review on the classification of organic/inorganic/carbonaceous hole transporting materials for perovskite solar cell application. *Arabian J Chem*. 2020;13(1):2526-2557. https://doi.org/10.1016/j.arabjc.2018.06.006

16. Kharangarh P, Misra D, Georgiou GE, Chin KK. Evaluation of Cu back contact related deep defects in CdTe solar cells. *ECS J Sol State Sci Technol*. 2012;1(5):Q110-Q113. https://doi.org/10.1149/2.001206jss

17. Capper P, ed. *Properties of Narrow Gap Cadmium-Based Compounds. EMIS Datareviews Series*. London: Institution of Electrical Engineers, INSPEC; 1994.

18. McCandless BE, Sites JR. Chapter 14: Cadmium telluride solar cells. In: Luque López A, Hegedus S, eds. *Handbook of Photovoltaic Science and Engineering*. Chichester: Wiley; 2011.

19. Kumar SG, Rao KSRK. Physics and chemistry of CdTe/CdS thin film heterojunction photovoltaic devices: fundamental and critical aspects. *Energy Environ Sci*. 2014;7(1):45-102. https://doi.org/10.1039/C3EE41981A

20. Znajdek K, Sibiński M, Kubiak A, Ruta Ł, Lisik Z, Janczak D. Analysis of back contact layers for flexible CdTe/CdS photovoltaic structures. *Opto-Electron Rev*. 2019;27(1):32-38. https://doi.org/10.1016/j.opelre.2018.12.001

21. Chou HC, Rohatgi A, Jokerst NM, Thomas EW, Kamra S. Copper migration in CdTe heterojunction solar cells. *JEM*. 1996;25(7):1093-1098. https://doi.org/10.1007/BF02659909

22. Phillips AB, Khanal RR, Song Z, et al. Wiring-up carbon single wall nanotubes to polycrystalline inorganic semiconductor thin films: low-barrier, copper-free back contact to CdTe solar cells. *Nano Lett*. 2013;13(11):5224-5232. https://doi.org/10.1021/nl402659c

23. Demtsu S, Albin D, Sites J. Role of copper in the performance of CdS/CdTe solar cells. In: *2006 IEEE 4th World Conference on Photovoltaic Energy Conference*. Waikoloa Village, HI: IEEE; 2006:523-526. https://doi.org/10.1109/WCPEC.2006.279507

24. Meyers PV, Liu CH, Russell L, et al. Polycrystalline CdTe on CuInSe2 cascaded solar cells. In: *Conference Record of the Twentieth IEEE Photovoltaic Specialists Conference*, Vol. 2. Las Vegas, NV: IEEE; 1988:1448-1451. https://doi.org/10.1109/PVSC.1988.105949

25. Cousins MA, Lane DW, Rogers KD. Sulphur diffusion in cadmium telluride thin films part 2: modelling grain-boundary diffusion. *Thin Solid Films*. 2003;431-432:78-83. https://doi.org/10.1016/S0040-6090(03)00206-2

26. Abbas A, Swanson D, Munshi A, et al. The effect of a post-activation annealing treatment on thin film CdTe device performance. In: *2015 IEEE 42nd Photovoltaic Specialist Conference (PVSC)*. New Orleans, LA: IEEE; 2015:1-6. https://doi.org/10.1109/PVSC.2015.7356441

27. Liyanage GK, Phillips AB, Alfadhili FK, Ellingson RJ, Heben MJ. The role of back buffer layers and absorber properties for >25% efficient CdTe solar cells. *ACS Appl Energy Mater*. 2019;2(8):5419-5426. https://doi.org/10.1021/acsaem.9b00367

28. Burgelman M, Nollet P, Degrave S. Modelling polycrystalline semiconductor solar cells. *Thin Solid Films*. 2000;361-362:527-532. https://doi.org/10.1016/S0040-6090(99)00825-1

29. Anthony TC, Fahrenbruch AL, Bube RH. Low resistance contacts to p-type cadmium telluride. *JEM*. 1982;11(1):89-109. https://doi.org/10.1007/BF02654611

30. Häring J-P, Werthen JG, Bube RH, Gulbrandsen L, Jansen W, Luscher P. Study of cleaved, oxidized, etched, and heat-treated CdTe surfaces. *J Vac Sci Technol A*. 1983;1(3):1469-1472. https://doi.org/10.1116/1.572170

31. Rimmaudo I, Salavei A, Artegiani E, et al. Improved stability of CdTe solar cells by absorber surface etching. *Sol Energy Mater Sol Cells*. 2017;162:127-133. https://doi.org/10.1016/j.solmat.2016.12.044

32. Awni RA, Grice CR, Li D, Song Z, Yan Y. Electrical impedance characterization of CdTe thin film solar cells with hydrogen iodide back surface etching. In: *2018 IEEE 7th World Conference on Photovoltaic Energy Conversion (WCPEC) (A Joint Conference of 45th IEEE PVSC, 28th PVSEC & 34th EU PVSEC)*. Waikoloa Village, HI: IEEE; 2018:1878-1881. https://doi.org/10.1109/PVSC.2018.8548289

33. Awni RA, Li D-B, Grice CR, et al. The effects of hydrogen iodide back surface treatment on CdTe solar cells. *Sol RRL*. 2019;3(3):1800304. https://doi.org/10.1002/solr.201800304

34. Li X, Niles DW, Hasoon FS, Matson RJ, Sheldon P. Effect of nitric-phosphoric acid etches on material properties and back-contact formation of CdTe-based solar cells. *J Vac Sci Technol A*. 1999;17(3):805-809. https://doi.org/10.1116/1.581651

35. Yan Y, Jones KM, Wu X, Al-Jassim MM. Microstructure of CdTe thin films after mixed nitric and phosphoric acids etching and (HgTe, CuTe)-graphite pasting. *Thin Solid Films*. 2005;472(1–2):291-296. https://doi.org/10.1016/j.tsf.2004.07.002

36. Song T, Sites JR. Role of tellurium buffer layer on CdTe solar cells' absorber/back-contact interface. In: *2017 IEEE 44th Photovoltaic Specialist Conference (PVSC)*. Washington, DC: IEEE. 2017:1308-1311. https://doi.org/10.1109/PVSC.2017.8366484

37. Proskuryakov YY, Durose K, Taele BM, Welch GP, Oelting S. Admittance spectroscopy of CdTe/CdS solar cells subjected to varied nitric-phosphoric etching conditions. *J Appl Phys*. 2007;101(1):014505. https://doi.org/10.1063/1.2402961

38. Major JD, Treharne RE, Phillips LJ, Durose K. A low-cost non-toxic post-growth activation step for CdTe solar cells. *Nature*. 2014;511(7509):334-337. https://doi.org/10.1038/nature13435

39. Hsiao K-J, Sites JR. Electron reflector strategy for CdTe solar cells. In: *2009 34th IEEE Photovoltaic Specialists Conference (PVSC)*. Philadelphia, PA: IEEE; 2009:1846-1850. https://doi.org/10.1109/PVSC.2009.5411531

40. Hsiao K-J, Sites JR. Electron reflector to enhance photovoltaic efficiency: application to thin-film CdTe solar cells: proposed electron reflector for CdTe solar cells. *Prog Photovolt Res Appl*. 2012;20(4):486-489. https://doi.org/10.1002/pip.1143

41. Swanson DE, Abbas A, Munshi AH, et al. Incorporation of $Cd_{1-x}Mg_xTe$ as an electron reflector for cadmium telluride photovoltaic cells. *MRS Proc*. 2015;1771:133-138. https://doi.org/10.1557/opl.2015.389

42. Ponpon JP. A Review of ohmic and rectifying contacts on cadmium telluride. *Solid-State Electron*. 1985;28(7):689-706. https://doi.org/10.1016/0038-1101(85)90019-X

43. Kaufmann U, Windscheif J, Brunthaler G. Identification of the isolated deep Ni acceptor in CdTe and ZnTe: comparison with isomorphous systems. *J Phys C: Sol State Phys*. 1984;17(34):6169-6176. https://doi.org/10.1088/0022-3719/17/34/017

44. Xia W, Lin H, Wu HN, et al. Te/Cu Bi-layer: a low-resistance back contact buffer for thin film CdS/CdTe solar cells. *Sol Energy Mater Sol Cells*. 2014;128:411-420. https://doi.org/10.1016/j.solmat.2014.06.010

45. Odkhuu D, Miao M, Aqariden F, Grein C, Kioussis N. Atomic and electronic structure of CdTe/Metal (Cu, Al, Pt) interfaces and their influence to the Schottky barrier. *J Appl Phys*. 2016;120(18):185703. https://doi.org/10.1063/1.4966931

46. Li S, Peng Z, Zheng J, Pan F. Optimizing CdTe–metal interfaces for high performance solar cells. *J Mater Chem A*. 2017;5(15):7118-7124. https://doi.org/10.1039/C7TA00698E

47. Niles DW, Li X, Sheldon P, Höchst H. A photoemission determination of the band diagram of the Te/CdTe interface. *J Appl Phys*. 1995;77(9):4489-4493. https://doi.org/10.1063/1.359444

48. Niles DW, Li X, Albin D, Rose D, Gessert T, Sheldon P. Evaporated Te on CdTe: a vacuum-compatible approach to making back contact to CdTe solar cell devices. *Prog Photovolt Res Appl*. 1996;4(3):225-229. https://doi.org/10.1002/(SICI)1099-159X(199605/06)4:3%3C225:AID-PIP122%3E3.0.CO;2-6

49. Kraft D, Thissen A, Broetz J, et al. Characterization of tellurium layers for back contact formation on close to technology treated CdTe surfaces. *J Appl Phys*. 2003;94(5):3589-3598. https://doi.org/10.1063/1.1597757

50. Moffett CE, Sampath WS. Characterization of tellurium as a back contact for CdTe solar cells. In: *2017 IEEE 44th Photovoltaic Specialist Conference (PVSC)*. Washington, DC: IEEE; 2017:2736-2739. https://doi.org/10.1109/PVSC.2017.8366272

51. Munshi AH, Kephart JM, Abbas A, et al. Polycrystalline CdTe photovoltaics with efficiency over 18% through improved absorber passivation and current collection. *Sol Energy Mater Sol Cells*. 2018;176:9-18. https://doi.org/10.1016/j.solmat.2017.11.031

52. Alfadhili FK, Phillips AB, Liyanage GK, Gibbs JM, Jamarkattel MK, Heben MJ. Controlling band alignment at the back interface of cadmium telluride solar cells using ZnTe and Te buffer layers. *MRS Adv*. 2019;4(16):913-919. https://doi.org/10.1557/adv.2019.31

53. Perrenoud J, Kranz L, Gretener C, et al. A comprehensive picture of Cu doping in CdTe solar cells. *J Appl Phys*. 2013;114(17):174505. https://doi.org/10.1063/1.4828484

54. Ferekides CS, Viswanathan V, Morel DL. RF sputtered back contacts for CdTe/CdS thin film solar cells. In: *Conference Record of the Twenty Sixth IEEE Photovoltaic Specialists Conference - 1997; PVSC*, Vol. 26. Anaheim, CA: IEEE; 1997:423-426. https://doi.org/10.1109/PVSC.1997.654118

55. McCandless BE, Hegedus SS, Birkmire RW, Cunningham D. Correlation of surface phases with electrical behavior in thin-film CdTe devices. *Thin Solid Films*. 2003;431–432:249-256. https://doi.org/10.1016/S0040-6090(03)00266-9

56. Avachat US. *Development of Transparent and Conducting Back Contacts on CdS/CdTe Solar Cells for Photoelectrochemical Application*. Masters thesis. USA: University of Central Florida; 2005.

57. Wu X, Zhou J, Duda A, et al. Phase control of Cu_xTe film and its effects on CdS/CdTe solar cell. *Thin Solid Films*. 2007;515(15):5798-5803. https://doi.org/10.1016/j.tsf.2006.12.151

58. Zhou J, Wu X, Duda A, Teeter G, Demtsu SH. The formation of different phases of Cu_xTe and their effects on CdTe/CdS solar cells. *Thin Solid Films*. 2007;515(18):7364-7369. https://doi.org/10.1016/j.tsf.2007.03.032

59. Moore A. *Performance and Metastability of CdTe Solar Cells with a Te Back-Contact Buffer Layer*. PhD thesis. Fort Collins, CO: Colorado State University; 2017.

60. Bosio A, Ciprian R, Lamperti A, et al. Interface phenomena between CdTe and ZnTe:Cu back contact. *Sol Energy*. 2018;176:186-193. https://doi.org/10.1016/j.solener.2018.10.035

61. Li J, Diercks DR, Ohno TR, et al. Controlled activation of ZnTe:Cu contacted CdTe solar cells using rapid thermal processing. *Sol Energy Mater Sol Cells*. 2015;133:208-215. https://doi.org/10.1016/j.solmat.2014.10.045

62. Janik E, Triboulet R. Ohmic contacts to P-type cadmium telluride and cadmium mercury telluride. *J Phys D: Appl Phys*. 1983;16(12):2333-2340. https://doi.org/10.1088/0022-3727/16/12/011

63. Zozime A, Vermeulin C. Properties of sputtered mercury telluride contacts on P-type cadmium telluride. *Rev Phys Appl (Paris)*. 1988;23(11):1825-1835. https://doi.org/10.1051/rphysap:0198800230110182500

64. Britt JS, Ferekides CS.US5557146A - Ohmic Contact Using Binder Paste with Semiconductor Material Dispersed Therein. US5557146A.

65. Duenow JN, Dhere RG, Li JV, Young MR, Gessert TA. Effects of back-contacting method and temperature on CdTe/CdS solar cells. In: *2010 35th IEEE Photovoltaic Specialists Conference*. Honolulu, HI: IEEE; 2010:1001-1005. https://doi.org/10.1109/PVSC.2010.5614593

66. Wu X, Keane JC, Dhere RG, et al. 16.5%-efficient CdS/CdTe polycrystalline thin-film solar cells. In: *17th EU-PVSEC; Munich, Germany*; 2001:995-1000.

67. Hanafusa A, Aramoto T, Morita A. Performance of graphite pastes doped with various materials as back contact for CdS/CdTe solar cell. *Jpn J Appl Phys*. 2001;40(Part 1, No. 12):6764-6769. https://doi.org/10.1143/JJAP.40.6764

68. Adachi S. *Optical Constants of Crystalline and Amorphous Semiconductors*. Boston, MA: Springer US; 1999. https://doi.org/10.1007/978-1-4615-5247-5

69. Van de Walle CG, Laks DB. Nitrogen doping in ZnSe and ZnTe. *Sol State Commun*. 1995;93(5):447-450. https://doi.org/10.1016/0038-1098(94)00815-9

70. Hishida Y, Ishii H, Toda T, Niina T. Growth and characterization of MBE-grown ZnTe:P. *J Cryst Growth*. 1989;95(1–4):517-521. https://doi.org/10.1016/0022-0248(89)90456-9

71. Oklobia O, Kartopu G, Irvine SJC. Properties of arsenic-doped ZnTe thin films as a back contact for CdTe solar cells. *Mater*. 2019;12(22):3706. https://doi.org/10.3390/ma12223706

72. Feldman RD, Austin RF, Sher A, et al. Antimony doping of ZnTe grown by molecular beam epitaxy. *J Cryst Growth*. 1992;118(3–4):295-298. https://doi.org/10.1016/0022-0248(92)90074-S

73. Späth B, Fritsche J, Klein A, Jaegermann W. P-ZnTe for back contacts to CdTe thin film solar cells. *MRS Proc*. 2005;865(F8):3. https://doi.org/10.1557/PROC-865-F8.3

74. Mondal A, McCandless BE, Birkmire RW. Electrochemical deposition of thin ZnTe films as a contact for CdTe solar cells. *Sol Energy Mater Sol Cells*. 1992;26(3):181-187. https://doi.org/10.1016/0927-0248(92)90059-X

75. Mahabaduge HP, Rance WL, Burst JM, et al. High-efficiency, flexible CdTe solar cells on ultra-thin glass substrates. *Appl Phys Lett*. 2015;106(13):133501. https://doi.org/10.1063/1.4916634

76. Amin N, Yamada A, Konagai M. Effect of ZnTe and CdZnTe alloys at the back contact of 1-μm-thick CdTe thin film solar cells. *Jpn J Appl Phys*. 2002;41(Part 1(5A)):2834-2841. https://doi.org/10.1143/JJAP.41.2834

77. Chen B, Liu J, Cai Z, et al. The effects of ZnTe:Cu back contact on the performance of CdTe nanocrystal solar cells with inverted structure. *Nanomater*. 2019;9(4):626. https://doi.org/10.3390/nano9040626

78. Gessert TA, Duenow JN, Ward S, Geisz JF, To B. Analysis of ZnTe:Cu/Ti contacts for crystalline CdTe. In: *IEEE 40th Photovoltaic Specialist Conference (PVSC)*. Denver, CO: IEEE; 2014:2329-2333. https://doi.org/10.1109/PVSC.2014.6925394

79. Ozawa M, Hiei F, Takasu M, Ishibashi A, Akimoto K. Low resistance ohmic contacts for *p*-type ZnTe. *Appl Phys Lett*. 1994;64(9):1120-1122. https://doi.org/10.1063/1.110825

80. Kurley JM, Panthani MG, Crisp RW, et al. Transparent ohmic contacts for solution-processed, ultrathin CdTe solar cells. *ACS Energy Lett*. 2017;2(1):270-278. https://doi.org/10.1021/acsenergylett.6b00587

81. Kurley JM. *Sintered Cadmium Telluride Nanocrystal Photovoltaics: Improving Chemistry to Facilitate Roll-to-Roll Fabrication*. PhD thesis. IL, USA: University of Chicago; 2017.

82. Feng Y, Wang T, Yu M, et al. Coevaporated $Cd_{1-x}Mg_xTe$ thin films for CdTe solar cells. *Renewable Energy*. 2020;145:13-20. https://doi.org/10.1016/j.renene.2019.05.139

83. Westrum EF, Chou C, Machol RE, Grønvold F. Thermodynamics of nonstoichiometric nickel tellurides. I. Heat capacity and thermodynamic functions of the δ phase from 5 to 350°K. *J Chem Phys*. 1958;28(3):497-503. https://doi.org/10.1063/1.1744164

84. Rotlevi O, Dobson KD, Rose D, Hodes G. Electroless Ni and $NiTe_2$ ohmic contacts for CdTe/CdS PV cells. *Thin Solid Films*. 2001;387:155-157.

85. Dobson KD, Rotlevi O, Rose D, Hodes G. Formation and characterization of electroless-deposited $NiTe_2$ back contacts to CdTe/CdS Thin-film solar cells. *J Electrochem Soc*. 2002;149(2):G147. https://doi.org/10.1149/1.1433752

86. Puotinen D, Newnham RE. The crystal structure of $MoTe_2$. *Acta Cryst*. 1961;14(6):691-692. https://doi.org/10.1107/S0365110X61002084

87. Dhar N, Chowdhury TH, Islam MA, et al. Effect of N-type transition metal dichalcogenide molybdenum telluride (n-$MoTe_2$) in back contact interface of cadmium telluride solar cells from numerical analysis. *Chalcog Lett*. 2014;11(6):271-279.

88. Moustafa M, Alzoubi T. Numerical study of CdTe solar cells with *p*-$MoTe_2$ TMDC as an interfacial layer using SCAPS. *Mod Phys Lett B*. 2018;32(23):1850269. https://doi.org/10.1142/S0217984918502699X

89. Dhar N, Khan NA, Chelvanathan P, et al. A comprehensive study on Mo/CdTe metal-semiconductor interface deposited by radio frequency magnetron sputtering. *J Nanosci Nanotechnol*. 2015;15(11):9291-9297. https://doi.org/10.1166/jnn.2015.11426

90. Löher T, Tomm Y, Pettenkofer C, Klein A, Jaegermann W. Structural dipoles at interfaces between polar II-VI semiconductors CdS and CdTe and non-polar layered transition metal dichalcogenide semiconductors $MoTe_2$ and WSe_2. *Semicond Sci Technol*. 2000;15(6):514-522. https://doi.org/10.1088/0268-1242/15/6/305

91. Shen D, Palekis V, Hodges D, et al. Tellurides as back contacts for substrate CdTe thin film solar cells on flexible foil substrates. In: *2010 35th IEEE Photovoltaic Specialists Conference*; Honolulu, HI: IEEE. 2010:1973-1976. https://doi.org/10.1109/PVSC.2010.5616594

92. Dey M, Matin MA, Das NK, Dey M. Germanium telluride as a BSF material for high efficiency ultra-thin CdTe solar cell. In: *2014 9th International Forum on Strategic Technology (IFOST)*. Cox's Bazar, Bangladesh: IEEE; 2014;334-338. https://doi.org/10.1109/IFOST.2014.6991134

93. Amps Modelling Software. http://www.ampsmodeling.org/

94. Höchst H, Niles DW, Engelhardt MA, Hernández-Calderón I. Strained-layer epitaxy of SnTe on CdTe(110). *J Vac Sci Technol A*. 1989;7(3):775-779. https://doi.org/10.1116/1.575838

95. Weng Z, Ma S, Zhu H, et al. CdTe thin film solar cells with a SnTe buffer layer in back contact. *Sol Energy Mater Sol Cells*. 2018;179:276-282. https://doi.org/10.1016/j.solmat.2017.12.018

96. Shu T, Xu H, Weng Z, Ma S, Wu H. Determination of band alignment at the CdTe/SnTe heterojunction interface for CdTe thin-film solar cells. *EPL*. 2019;127(3):37003. https://doi.org/10.1209/0295-5075/127/37003

97. Matin MA, Dey M. High performance ultra-thin CdTe solar cell with lead telluride BSF. In: *2014 International Conference on Informatics, Electronics & Vision (ICIEV)*. Dhaka, Bangladesh: IEEE; 2014:1-5. https://doi.org/10.1109/ICIEV.2014.6850826

98. Si J, Jin S, Zhang H, Zhu P, Qiu D, Wu H. Experimental determination of valence band offset at PbTe/CdTe(111) heterojunction interface by X-ray photoelectron spectroscopy. *Appl Phys Lett*. 2008;93(20):202101. https://doi.org/10.1063/1.3028028

99. Swartz CH, Rab SR, Paul S, et al. Measurement of band offsets and shunt resistance in CdTe solar cells through temperature and intensity dependence of open circuit voltage and photoluminescence. *Sol Energy*. 2019;189:389-397. https://doi.org/10.1016/j.solener.2019.07.057

100. Panchuk O, Savitskiy A, Fochuk P, et al. IV group dopant compensation effect in CdTe. *J Cryst Growth*. 1999;197(3):607-611. https://doi.org/10.1016/S0022-0248(98)00798-2

101. Itoh K, Mizuhara Y, Otomo T. Mechanochemical synthesis of binary phosphorus telluride: short range structure and thermal properties. *J Sol State Chem*. 2018;267:119-123. https://doi.org/10.1016/j.jssc.2018.08.018

102. Oehling S, Lugauer HJ, Schmitt M, et al. *P*-type doping of CdTe with a nitrogen plasma source. *J Appl Phys*. 1996;79(5):2343-2346. https://doi.org/10.1063/1.361160

103. Alnajjar A. *Single Crystal CdS-CdTe: P Solar Cells*. PhD thesis. UK: Durham University; 1992.

104. Barrioz V, Proskuryakov YY, Jones EW, et al. Highly arsenic doped cdte layers for the back contacts of CdTe solar cells. *MRS Proc*. 2007;1012:1012–Y12-08. https://doi.org/10.1557/PROC-1012-Y12-08

105. Zhao H, Razykov TM, Hodges D, et al. Introduction of Sb in CdTe and its effect on cdte solar cells. In: *2008 33rd IEEE Photovoltaic Specialists Conference*. San Diego, CA: IEEE; 2008:1-5. https://doi.org/10.1109/PVSC.2008.4922554

106. Shahil KMF, Hossain MZ, Goyal V, Balandin AA. Micro-Raman spectroscopy of mechanically exfoliated few-quintuple layers of Bi_2Te_3, Bi_2Se_3, and Sb_2Te_3 materials. *J Appl Phys*. 2012;111(5):054305. https://doi.org/10.1063/1.3690913

107. Romeo N, Bosio A, Tedeschi R, Canevari V. back contacts to CSS CdS/CdTe solar cells and stability of performances. *Thin Solid Films*. 2000;361–362:327-329. https://doi.org/10.1016/S0040-6090(99)00765-8

108. Paudel NR, Wieland KA, Nawarange AV, et al. Studies of RF sputtered Sb_2Te_3 thin fislms for back contacts to CdS/CdTe solar cells. In: *2011 37th IEEE Photovoltaic Specialists Conference*. Seattle, WA: IEEE; 2011:1342-1345. https://doi.org/10.1109/PVSC.2011.6186206

109. Al Turkestani MK. *CdTe Solar Cells; Key Layers & Electrical Effects*. PhD thesis. UK: Durham University; 2010.

110. Romeo N, Bosio A, Romeo A. An innovative process suitable to produce high-efficiency CdTe/CdS thin-film modules. *Sol Energy Mater Sol Cells*. 2010;94(1):2-7. https://doi.org/10.1016/j.solmat.2009.06.001

111. Romeo N, Bosio A, Rosa G. The back contact in CdTe/CdS thin film solar cells. In: *Proceedings of SWC2017/SHC2017*. Abu Dhabi: International Solar Energy Society; 2017:1-3. https://doi.org/10.18086/swc.2017.20.08

112. Lee K-K, Myers TH. Band structure measurement and analysis of the Bi_2Te_3/CdTe (111) *B* heterojunction. *J Vac Sci Technol A*. 2015;33(3):031602. https://doi.org/10.1116/1.4914175

113. Romeo A, Salavei A, Rimmaudo I, et al. Electrical characterization and aging of CdTe thin film solar cells with Bi2Te3 back contact. In: *2013 IEEE 39th Photovoltaic Specialists Conference (PVSC)*. Tampa, FL: IEEE; 2013:1178-1182. https://doi.org/10.1109/PVSC.2013.6744350

114. Tang R, Wang Z, Li W, et al. Bi_2Te_3 thin films prepared by co-evaporation for CdTe thin film solar cells. *Sol Energy Mater Sol Cells*. 2014;121:92-98. https://doi.org/10.1016/j.solmat.2013.10.039

115. Kraft D, Weiler U, Tomm Y, Thissen A, Klein A, Jaegermann W. Alternative back contacts for CdTe solar cells: a photoemission study of the VSe_2/CdTe and $TiSe_2$/CdTe interface formation. *Thin Solid Films*. 2003;431–432:382-386. https://doi.org/10.1016/S0040-6090(03)00254-2

116. Zhao H. *Impurity and Back Contact Effects on CdTe/CdS Thin Film Solar Cells*. PhD. University of South Florida, FL, USA; 2007.

117. Ferekides CS, Morel DL. *Process Development for High Voc CdTe Solar Cells; Sub-contract Report NREL/SR-5200-51605, 1016430*. University of South Florida; 2011:43. https://doi.org/10.2172/1016430

118. Glazov VM, Pashinkin AS, Fedorov VA. Phase equilibria in the Cu-Se system. *Inorg Mater*. 2000;36(7):641-652. https://doi.org/10.1007/BF02758413

119. Kuroda S, Minami K, Takita K. Epitaxial growth of II–VI semiconductor CdTe on a layered material $NbSe_2$. *J Cryst Growth*. 2004;262(1–4):383-387. https://doi.org/10.1016/j.jcrysgro.2003.10.048

120. Gao J, Di X, Li W, et al. Preparation of vanadium diselenide thin films and their application in CdTe solar cells. *Thin Solid Films*. 2014;550:638-642. https://doi.org/10.1016/j.tsf.2013.10.032

121. Weirich TE, Simon A, Pöttgen R. Ti9Se2 - eine verbindung mit kolumnaren. *ZAAC*. 1996;622(4):630-634. https://doi.org/10.1002/zaac.19966220410

122. Weirich TE, Ramlau R, Simon A, Hovmöller S, Zou X. A crystal structure determined with 0.02 Å accuracy by electron microscopy. *Nature*. 1996;382(6587):144-146. https://doi.org/10.1038/382144a0

123. Murray JL. The Se−Ti (selenium-titanium) system. *Bull Alloy Phase Diag*. 1986;7(2):163-165. https://doi.org/10.1007/BF02881556

124. Kim D, McCandless BE, Hegedus S, Birkmire RW. Cu_xS Back Contact for CdTe Solar Cells. Osaka, Japan: IEEE; 2003:4.

125. Lei Z, Feng L, Zeng G, et al. Influence of Cu_xS back contact on CdTe thin film solar cells. *J Semicond*. 2013;34(1):014008. https://doi.org/10.1088/1674-4926/34/1/014008

126. Türck J, Siol S, Mayer T, Klein A, Jaegermann W. Cu_2S as ohmic back contact for CdTe solar cells. *Thin Solid Films*. 2015;582:336-339. https://doi.org/10.1016/j.tsf.2014.11.017

127. Subedi KK, Bhandari KP, Bastola E, Ellingson RJ. 13% CdS/CdTe solar cell using a nanocomposite (CuS)x(ZnS)1-x thin film hole transport layer. In: *2017 IEEE 44th Photovoltaic Specialist Conference (PVSC)*. Washington, DC: IEEE; 2017:781-784. https://doi.org/10.1109/PVSC.2017.8366719

128. Zakutayev A, Woods-Robinson R, Ablekim T, et al. Sputtered P-type $Cu_xZn_{1-x}S$ back contact to CdTe solar cells. *ACS Appl Energy Mater*. 2020. https://doi.org/10.1021/acsaem.0c00413

129. Bhandari KP, Koirala P, Paudel NR, et al. Iron pyrite nanocrystal film serves as a copper-free back contact for polycrystalline CdTe thin film solar cells. *Sol Energy Mater Sol Cells*. 2015;140:108-114. https://doi.org/10.1016/j.solmat.2015.03.032

130. Bhandari KP, Tan X, Zereshki P, et al. Thin film iron pyrite deposited by hybrid sputtering/co-evaporation as a hole transport layer for sputtered CdS/CdTe solar cells. *Sol Energy Mater Sol Cells*. 2017;163:277-284. https://doi.org/10.1016/j.solmat.2017.01.044

131. Bhandari KP, Roland PJ, Koirala P, et al. Enhancing the efficiency of CdTe solar cells using a nanocrystalline iron pyrite film as an interface layer. In: *2015 IEEE 42nd Photovoltaic Specialist Conference (PVSC)*. New Orleans, LA: IEEE; 2015:1-4. https://doi.org/10.1109/PVSC.2015.7356104

132. Bhandari KP, Tan X, Zereshki P, Collins RW, Ellingson RJ. *CdTe Solar Cells with Thin Film Iron Pyrite Back Contacts Fabricated by a Hybrid Sputtering/Co-Evaporation Process; PVSC*. Portland, OR: IEEE; 2016. https://doi.org/10.1109/PVSC.2016.7749851

133. Bastola E, Bhandari KP, Subedi I, Podraza NJ, Ellingson RJ. Structural, optical, and hole transport properties of earth-abundant chalcopyrite (CuFeS2) nanocrystals. *MRS Commun*. 2018;8(03):970-978. https://doi.org/10.1557/mrc.2018.117

134. Bastola E, Bhandari KP, Ellingson RJ. Application of composition controlled nickel-alloyed iron sulfide pyrite nanocrystal thin films as the hole transport layer in cadmium telluride solar cells. *J Mater Chem C*. 2017;5(20):4996-5004. https://doi.org/10.1039/C7TC00948H

135. Pitchaiya S, Natarajan M, Santhanam A, et al. Nickel sulphide-carbon composite hole transporting material for $(CH_3NH_3PbI_3)$ planar heterojunction perovskite solar cell. *Mater Lett*. 2018;221:283-288. https://doi.org/10.1016/j.matlet.2018.03.161

136. Subedi KK, Bastola E, Subedi I, et al. Bifacial CdS/CdTe solar cell using transparent barium copper sulfide as a hole transport layer. In: *2019 IEEE 46th Photovoltaic Specialists Conference (PVSC)*. Chicago, IL: IEEE; 2019:4. https://doi.org/10.1109/PVSC40753.2019.8980936

137. Tan X. *Applications of Multichannel Spectroscopic Ellipsometry for CdTe Photovoltaics: From Window Layers to Back Contacts*. PhD. University of Toledo, USA; 2017.

138. Yuan S, Zhang M-J, Yang X, Mei Z, Chen Y, Pan F. A novel MoS_2-based hybrid film as the back electrode for high-performance thin film solar cells. *RSC Adv*. 2017;7(38):23415-23421. https://doi.org/10.1039/C7RA03233A

139. Deng X-Z, Zhang J-R, Zhao Y-Q, Yu Z-L, Yang J-L, Cai M-Q. The energy band engineering for the high-performance infrared photodetectors constructed by $CdTe/MoS_2$ heterojunction. *J Phys: Cond Matter*. 2020;32(6):065004. https://doi.org/10.1088/1361-648X/ab4013

140. Gong C, Colombo L, Wallace RM, Cho K. The unusual mechanism of partial fermi level pinning at metal–MoS_2 interfaces. *Nano Lett*. 2014;14(4):1714-1720. https://doi.org/10.1021/nl403465v

141. Clayton AJ, Baker MA, Babar S, et al. Effects of $Cd_{1-x}Zn_xS$ alloy composition and post-deposition air anneal on ultra-thin CdTe solar cells produced by MOCVD. *Mater Chem Phys*. 2017;192:244-252. https://doi.org/10.1016/j.matchemphys.2017.01.067

142. Major JD. Grain boundaries in CdTe thin film solar cells: a review. *Semicond Sci Technol*. 2016;31(9):093001. https://doi.org/10.1088/0268-1242/31/9/093001

143. Crossay A, Buecheler S, Kranz L, et al. Spray-deposited Al-doped ZnO transparent contacts for CdTe solar cells. *Sol Energy Mater Sol Cells*. 2012;101:283-288. https://doi.org/10.1016/j.solmat.2012.02.008

144. Parikh VY. *Studies of Two-Terminal and Four-Terminal Polycrystalline Thin Film Tandem Solar Cells Based on II-VI Materials*. PhD. University of Toledo, USA; 2007.

145. Heisler C, Schnohr CS, Hädrich M, et al. Transparent CdTe solar cells with a ZnO:Al back contact. *Thin Solid Films*. 2013;548:627-631. https://doi.org/10.1016/j.tsf.2013.09.087

146. Duenow JN, Barnes TM, Dhere RG, et al. Comparison of transparent back contacts for CdTe top cells in tandem thin-film photovoltaic devices. In: *2009 34th IEEE Photovoltaic Specialists Conference (PVSC)*. Philadelphia, PA: IEEE; 2009:2443-2447. https://doi.org/10.1109/PVSC.2009.5411282

147. Calnan S. *Growth and Characterisation of Sputtered Transparent Conducting Oxides Targeting Improved Solar Cell Efficiency*. PhD thesis. UK: Loughborough University; 2008.

148. Calnan S, Uphadhyaya HM, Buecheler S, et al. Application of high mobility transparent conductors to enhance long wavelength transparency of the intermediate solar cell in multi-junction solar cells. *Thin Solid Films*. 2009;517(7):2340-2343. https://doi.org/10.1016/j.tsf.2008.11.007

149. Romeo A, Khrypunov G, Galassini S, Zogg H, Tiwari AN. Bifacial configurations for CdTe solar cells. *Sol Energy Mater Sol Cells*. 2007;91(15–16):1388-1391. https://doi.org/10.1016/j.solmat.2007.03.010

150. Crisp RW, Panthani MG, Rance WL, et al. Nanocrystal grain growth and device architectures for high-efficiency CdTe ink-based photovoltaics. *ACS Nano*. 2014;8(9):9063-9072. https://doi.org/10.1021/nn502442g

151. Guo Y, Robertson J. Origin of the high work function and high conductivity of MoO_3. *Appl Phys Lett*. 2014;105(22):222110. https://doi.org/10.1063/1.4903538

152. Perrenoud J. *Low Temperature Grown CdTe TFSCs on Flexible Substrates*. PhD, ETHZ, Zurich, Switzerland; 2012.

153. Gretener C. *Back Contact, Doping & Stability of CdTe Thin Film Solar Cells in Substrate Configuration*. PhD, ETHZ, Zurich, Switzerland; 2015.

154. Zhang M, Qiu L, Li W, Zhang J, Wu L, Feng L. Copper doping of MoO thin films for CdTe solar cells. *Mater Sci Semicond Process*. 2018;86:49-57. https://doi.org/10.1016/j.mssp.2018.06.008

155. Lin H, Irfan XW, Wu HN, Gao Y, Tang CW. MoO_x back contact for CdS/CdTe thin film solar cells: preparation, device characteristics, and stability. *Sol Energy Mater Sol Cells*. 2012;99:349-355. https://doi.org/10.1016/j.solmat.2012.01.001

156. Lin H. *Study of Molybdenum Oxide as a Back Contact Buffer for Thin Film N-CdS/p-CdTe Solar Cells*. PhD thesis. USA: University of Rochester; 2012.

157. Artegiani E. *New Paradigms for Advances in Efficiency and Stability of CdTe Solar Cells*. PhD thesis. Italy: Univeristy of Verona; 2019.

158. Paudel NR, Yan Y. Valence band offset at MoO3/CdTe interface probed by X-ray photoelectron spectroscopy. In: *2014 IEEE 40th Photovoltaic Specialist Conference (PVSC)*. Denver, CO: IEEE. 2014:2397-2399. https://doi.org/10.1109/PVSC.2014.6925410

159. Drayton JA, Williams DD, Geisthardt RM, Cramer CL, Williams JD, Sites JR. Molybdenum oxide and molybdenum oxide-nitride back contacts for CdTe solar cells. *J Vac Sci Technol A*. 2015;33(4):041201. https://doi.org/10.1116/1.4922576

160. Lemmon JP, Polikarpov E, Bennett WD, Kovarik L. Thin metal oxide films to modify a window layer in CdTe-based solar cells for improved performance. *Appl Phys Lett*. 2012;100(21):213908. https://doi.org/10.1063/1.4722921

161. Kumar S, Qadir A, Maury F, Bahlawane N. Visible thermochromism in vanadium pentoxide coatings. *ACS Appl Mater Interfaces*. 2017;9(25):21447-21456. https://doi.org/10.1021/acsami.7b04484

162. Bremond G, Zerrai A, Marrakchi G, et al. Characterization and identification of the deep levels in V doped CdTe and their relationship with the photorefractive properties. *Opt Mater*. 1995;4(2–3):246-251. https://doi.org/10.1016/0925-3467(94)00068-9

163. Paudel NR, Xiao C, Yan Y. CdS/CdTe thin-film solar cells with Cu-free transition metal oxide/Au back contacts: CdTe cells with Cu-free TMO/Au back contacts. *Prog Photovolt Res Appl*. 2015;23(4):437-442. https://doi.org/10.1002/pip.2446

164. Shen K, Yang R, Wang D, et al. Stable CdTe solar cell with V2O5 as a back contact buffer layer. *Sol Energy Mater Sol Cells*. 2016;144:500-508. https://doi.org/10.1016/j.solmat.2015.09.036

165. Ishikawa R, Furuya Y, Araki R, et al. Preparation of P-type NiO films by reactive sputtering and their application to CdTe solar cells. *Jpn J Appl Phys*. 2016;55(2S):02BF04. https://doi.org/10.7567/JJAP.55.02BF04

166. Xiao D, Li X, Wang D, Li Q, Shen K, Wang D. CdTe thin film solar cell with NiO as a back contact buffer layer. *Sol Energy*

Mater Sol Cells. 2017;169:61-67. https://doi.org/10.1016/j.solmat.2017.05.006

167. Owings RR, Exarhos GJ, Windisch CF, Holloway PH, Wen JG. Process enhanced polaron conductivity of infrared transparent nickel-cobalt oxide. *Thin Solid Films*. 2005;483(1–2):175-184. https://doi.org/10.1016/j.tsf.2005.01.011

168. Tiefenbacher S, Pettenkofer C, Jaegermann W. Ultrahigh vacuum preparation and characterization of TiO$_2$/CdTe interfaces: electrical properties and implications for solar cells. *J Appl Phys*. 2002;91(4):1984-1987. https://doi.org/10.1063/1.1435413

169. Brus VV, Ilashchuk MI, Kovalyuk ZD, Maryanchuk PD. Light-dependent *I-V* characteristics of TiO$_2$/CdTe heterojunction solar cells. *Semicond Sci Technol*. 2012;27(5):055008. https://doi.org/10.1088/0268-1242/27/5/055008

170. Schwarz R, Joerger W, Eiche C, Fiederle M, Benz KW. Closed tube vapour growth of CdTe:V and CdTe:Ti and its characterization. *J Cryst Growth*. 1995;146(1–4):92-97. https://doi.org/10.1016/0022-0248(94)00472-2

171. Fu R, Pattison J, Chen A, Nayfeh O. In: Andresen BF, Fulop GF, Norton PR, eds. *Mercury Cadmium Telluride (HgCdTe) Passivation by Advanced Thin Conformal Al2O3 Films*. Baltimore, MD, USA; 2012:83532I–83532I–7. https://doi.org/10.1117/12.918605

172. Dingemans G, Kessels WMM. Status and prospects of Al$_2$O$_3$-based surface passivation schemes for silicon solar cells. *J Vac Sci Technol A*. 2012;30(4):040802. https://doi.org/10.1116/1.4728205

173. Vermang B, Wätjen JT, Fjällström V, et al. Employing Si solar cell technology to increase efficiency of ultra-thin Cu(In, Ga)S$_e$2 solar cells: employing Si solar cell technology. *Prog Photovolt Res Appl*. 2014;22(10):1023-1029. https://doi.org/10.1002/pip.2527

174. Kephart JM, Kindvall A, Williams D, et al. Sputter-deposited oxides for interface passivation of CdTe photovoltaics. *IEEE J Photovoltaics*. 2018;8(2):587-593. https://doi.org/10.1109/JPHOTOV.2017.2787021

175. Su Y, Xin C, Feng Y, et al. Band alignment for rectification and tunneling effects in Al$_2$O$_3$ atomic-layer-deposited on back contact for CdTe solar cell. *ACS Appl Mater Interfaces*. 2016;8(41):28143-28148. https://doi.org/10.1021/acsami.6b07421

176. Zeng G, Hao X, Ren S, Feng L, Wang Q. Application of ALD-Al$_2$O$_3$ in CdS/CdTe thin-film solar cells. *Energies*. 2019;12(6):1123. https://doi.org/10.3390/en12061123

177. Liang J, Lin Q, Li H, et al. Rectification and tunneling effects enabled by Al$_2$O$_3$ atomic layer deposited on back contact of CdTe solar cells. *Appl Phys Lett*. 2015;107(1):013907. https://doi.org/10.1063/1.4926601

178. Lin Q, Su Y, Zhang M-J, et al. A novel P-type and metallic dual-functional Cu–Al$_2$O$_3$ ultra-thin layer as the back electrode enabling high performance of thin film solar cells. *Chem Commun*. 2016;52(71):10708-10711. https://doi.org/10.1039/C6CC04299F

179. Munshi AH, Danielson AH, Kindvall A, Barth K, Sampath W. Investigation of sputtered oxides and p+ back-contact for polycrystalline CdTe and CdSeTe photovoltaics. In: *2018 IEEE 7th World Conference on Photovoltaic Energy Conversion (WCPEC) (A Joint Conference of 45th IEEE PVSC, 28th PVSEC & 34th EU PVSEC)*. Waikoloa Village, HI: IEEE; 2018:3009-3012. https://doi.org/10.1109/PVSC.2018.8548203

180. Meyer BK, Polity A, Reppin D, et al. Binary copper oxide semiconductors: from materials towards devices. *Phys Stat Sol B*. 2012;249(8):1487-1509. https://doi.org/10.1002/pssb.201248128

181. Ghosh B, Mondal NK, Banerjee P, Pal J, Das S. A method for forming low resistance contact to P-CdTe. *IEEE Trans Electron Dev*. 2002;49(12):2352-2355. https://doi.org/10.1109/TED.2002.805616

182. Türck J, Nonnenmacher H-J, Connor PML, et al. Copper (I) oxide (Cu$_2$O) based back contact for p-i-n CdTe solar cells. *Prog Photovolt Res Appl*. 2016;24(9):1229-1236. https://doi.org/10.1002/pip.2782

183. Masood HT, Shen K, Li Q, Xiao D, Wang D. CdTe thin film solar cells fabricated with CuO as a buffer layer in the back contact. *IEEE J Photovoltaics*. 2017;7(4):1124-1129. https://doi.org/10.1109/JPHOTOV.2017.2689163

184. Chen Y-J, Li M-H, Huang J-C-A, Chen P. Cu/Cu$_2$O nanocomposite films as a p-type modified layer for efficient perovskite solar cells. *Sci Rep*. 2018;8(1):7646. https://doi.org/10.1038/s41598-018-25975-8

185. Yang Z, Koirala P, Collins RW, et al. Transition metal nitride contacts for CdTe photovoltaics. In: *2014 IEEE 40th Photovoltaic Specialist Conference (PVSC)*. Denver, CO: IEEE; 2014:1735-1739. https://doi.org/10.1109/PVSC.2014.6925256

186. Guntur V. *Molybdenum Nitride Films in the Back Contact Structure of Flexible Substrate CdTe Solar Cells*. Masters thesis. USA: University of South Florida; 2011.

187. Kindvall A, Kephart J, Sampath W. Molybdenum oxide and molybdenum nitride back contacts for thin-film CdTe solar cells. In: *2017 IEEE 44th Photovoltaic Specialist Conference (PVSC); PVSC*. Washington, DC: IEEE; 2017:785-790. https://doi.org/10.1109/PVSC.2017.8366271

188. Malmström J, Schleussner S, Stolt L. Enhanced back reflectance and quantum efficiency in Cu(In, Ga)S$_e$2 thin film solar cells with a ZrN back reflector. *Appl Phys Lett*. 2004;85(13):2634-2636. https://doi.org/10.1063/1.1794860

189. Uličná S, Arnou P, Abbas A, et al. Deposition and application of a Mo–N back contact diffusion barrier yielding a 12.0% efficiency solution-processed CIGS solar cell using an amine-thiol solvent system. *J Mater Chem A*. 2019;7(12):7042-7052. https://doi.org/10.1039/C8TA12089G

190. Viswanathan V, Tetali B, Selvaraj P,, et al. Ni2P-a promising candidate for back contacts to CdS/CdTe solar cells. In: *Conference Record of the Twenty-Eighth IEEE Photovoltaic Specialists Conference - 2000 (Cat. No.00CH37036)*. Anchorage, AK: IEEE; 2000:587-590. https://doi.org/10.1109/PVSC.2000.915908

191. Yanagi H, Park S, Draeseke AD, Keszler DA, Tate J. P-type conductivity in transparent oxides and sulfide fluorides. *J Sol State Chem*. 2003;175(1):34-38. https://doi.org/10.1016/S0022-4596(03)00095-1

192. Spies JA. *Inorganic Thin-Film Solar Cells*. Masters thesis. OR, USA: Oregon State University; 2007.

193. Yamamoto K, Okamoto H, Sakakima H, et al. Fabrication of transparent P-type conductive BaCuSeF films by pulsed laser deposition and their application to CdS/CdTe solar cells. *Jpn J Appl Phys*. 2014;53(5S1):05FX02. https://doi.org/10.7567/JJAP.53.05FX02

194. Yamamoto K, Sakakima H, Ogawa Y, Hosono A, Okamoto T, Wada T. Fabrication of CdS/CdTe solar cells with transparent p-type conductive BaCuSeF back contact. *Jpn J*

Appl Phys. 2015;54(8S1):08KC01. https://doi.org/10.7567/JJAP.54.08KC01

195. Kitabayashi S, Shiina Y, Murata A, Okamoto T, Wada T. Fabrication of P-type SrCuSeF/n-type In$_2$O$_3$:Sn bilayer ohmic tunnel junction and its application to the back contact of CdS/CdTe solar cells. *Jpn J Appl Phys* 2017;56(8S2):08MC18. https://doi.org/10.7567/JJAP.56.08MC18

196. Wada T, Miki K, Tamai D, et al. Fabrication of P-type Na doped SrCuSeF & n-type ITO bilayer ohmic tunnel junction as back contact of CdTe SC. *EU-PVSEC*. 2018;35:3BV.2.36.

197. Miki K, Kawabe T, Shiina Y, Okamoto S, Okamoto T, Wada T. Fabrication of P-type BaCuSF and n-Type In$_2$O$_3$:Sn bilayer films and their applications to the back contact of CdS/CdTe solar cells. *Jpn J Appl Phys*. 2018;57(8S3):08RC19. https://doi.org/10.7567/JJAP.57.08RC19

198. Bhandari KP, Watthage SC, Song Z, et al. Applications of hybrid organic-inorganic metal halide perovskite thin film as a hole transport layer in CdTe thin film solar cells. In: *2017 IEEE 44th Photovoltaic Specialist Conference (PVSC)*. Washington, DC: IEEE; 2017:748-751. https://doi.org/10.1109/PVSC.2017.8366784

199. Liyanage GK, Phillips AB, Alfadhili FK, et al. Modeling the performance of CdTe solar cells with a CH3NH3Pb(I1-xBrx)3-like back buffer layer. In: *2018 IEEE 7th World Conference on Photovoltaic Energy Conversion (WCPEC) (A Joint Conference of 45th IEEE PVSC, 28th PVSEC & 34th EU PVSEC)*. Waikoloa Village, HI: IEEE; 2018:1503-1506. https://doi.org/10.1109/PVSC.2018.8548092

200. Li X, Xiao D, Wu L, Wang D, Wang G, Wang D. CdTe thin film solar cells with copper iodide as a back contact buffer layer. *Sol Energy*. 2019;185:324-332. https://doi.org/10.1016/j.solener.2019.04.082

201. Artegiani E, Menossi D, Shiel H, et al. Analysis of a novel CuCl$_2$ back contact process for improved stability in CdTe solar cells. *Prog Photovolt Res Appl*. 2019;27(8):706-715. https://doi.org/10.1002/pip.3148

202. Shi Z, Jayatissa A. The impact of graphene on the fabrication of thin film solar cells: current status and future prospects. *Mater*. 2017;11(1):36. https://doi.org/10.3390/ma11010036

203. Liang J, Bi H, Wan D, Huang F. Novel Cu nanowires/graphene as the back contact for CdTe solar cells. *Adv Funct Mater*. 2012;22(6):1267-1271. https://doi.org/10.1002/adfm.201102809

204. Lin T, Huang F, Liang J, Wang Y. A facile preparation route for boron-doped graphene, and Its CdTe solar cell application. *Energy Environ Sci*. 2011;4(3):862-865. https://doi.org/10.1039/C0EE00512F

205. Barnes TM, Wu X, Zhou J, et al. Single-wall carbon nanotube networks as a transparent back contact in CdTe solar cells. *Appl Phys Lett*. 2007;90(24):243503. https://doi.org/10.1063/1.2748078

206. Khanal RR. *Carbon Single Wall Nanotubes: Low Barrier, Cu-Free Back Contact to CdTe Based Solar*. PhD thesis. Toledo, OH, USA: University of Toledo; 2014.

207. Li B, Zhou H, Li H, Liu X. Enriched semiconducting single wall nanotubes as back contact for CdTe solar cell. In: *2016 IEEE 11th Annual International Conference on Nano/Micro Engineered and Molecular Systems (NEMS)*. Sendai, Japan: IEEE; 2016:107-110. https://doi.org/10.1109/NEMS.2016.7758210

208. Alfadhili FK, Gibbs JM, Liyanage GK, et al. Use of single wall carbon nanotube films doped with triethyloxonium hexachlorantimonate as a transparent back contact for CdTe solar cells. In: *2017 IEEE 44th Photovoltaic Specialist Conference (PVSC)*. Washington, DC: IEEE; 2017:730-734. https://doi.org/10.1109/PVSC.2017.8366121

209. Koirala P, Huang Z, Junda M, et al. Investigation of doped A-Si1-xCx:H as a novel back contact material for CdTe solar cells. In: *2014 IEEE 40th Photovoltaic Specialist Conference (PVSC); PVSC*. Denver, CO: IEEE; 2014:2354-2359. https://doi.org/10.1109/PVSC.2014.6925399

210. Paudel NR, Yan Y. Application of copper thiocyanate for high open-circuit voltages of CdTe solar cells: application of copper thiocyanate. *Prog Photovolt Res Appl*. 2016;24(1):94-101. https://doi.org/10.1002/pip.2660

211. Tena-Zaera R, Katty A, Bastide S, Lévy-Clément C, O'Regan B, Muñoz-Sanjosé V. ZnO/CdTe/CuSCN, a promising heterostructure to act as inorganic eta-solar cell. *Thin Solid Films*. 2005;483(1–2):372-377. https://doi.org/10.1016/j.tsf.2005.01.010

212. Wijeyasinghe N, Regoutz A, Eisner F, et al. Copper(I) thiocyanate (CuSCN) hole-transport layers processed from aqueous precursor solutions and their application in thin-film transistors and highly efficient organic and organometal halide perovskite solar cells. *Adv Funct Mater*. 2017;27(35):1701818. https://doi.org/10.1002/adfm.201701818

213. Arora N, Dar MI, Hinderhofer A, et al. Perovskite solar cells with CuSCN hole extraction layers yield stabilized efficiencies greater than 20%. *Science*. 2017;358(6364):768-771. https://doi.org/10.1126/science.aam5655

214. Pressman AB. *Electrical Properties of Cadmium Telluride Thin Film Solar Cells Activated with Magnesium Chloride*. PhD. University of Liverpool, UK; 2017.

215. Montgomery A, Guo L, Grice C, et al. Solution-processed copper (I) thiocyanate (CuSCN) for highly efficient CdSe/CdTe thin-film solar cells. *Prog Photovolt Res Appl*. 2019;27:665-672. https://doi.org/10.1002/pip.3136

216. Yan F, Guo L, Montgomery A. Application of solution-processed CuSCN and AgSCN for highly efficient cdte solar cells. In: *PVSC*. Chicago, IL: IEEE; 2019.

217. Cohen R, Bastide S, Cahen D, Libman J, Shanzer A, Rosenwaks Y. Controlling electronic properties of CdTe by adsorption of dicarboxylic acid derivatives: relating molecular parameters to band bending and electron affinity changes. *Adv Mater*. 1997;9(9):746-749. https://doi.org/10.1002/adma.19970090915

218. Cohen R, Bastide S, Cahen D, Libman J, Shanzer A, Rosenwaks Y. Controlling surfaces and interfaces of semiconductors using organic molecules. *Opt Mater*. 1998;9(1–4):394-400. https://doi.org/10.1016/S0925-3467(97)00065-7

219. Jarkov A, Bereznev S, Laes K, et al. Conductive polymer PEDOT:PSS back contact for CdTe solar cell. *Thin Solid Films*. 2011;519(21):7449-7452. https://doi.org/10.1016/j.tsf.2010.12.230

220. Wang W, Paudel NR, Yan Y, Duarte F, Mount M. PEDOT:PSS as back contact for CdTe solar cells and the effect of PEDOT:PSS conductivity on device performance. *J Mater Sci: Mater Electron*. 2016;27(2):1057-1061. https://doi.org/10.1007/s10854-015-3850-1

221. Jarkov A, Bereznev S, Volobujeva O, et al. Photo-assisted electrodeposition of polypyrrole back contact to CdS/CdTe solar cell structures. *Thin Solid Films*. 2013;535:198-201. https://doi.org/10.1016/j.tsf.2013.01.064

222. Koll DK, Taha AH, Giolando DM. Photochemical "self-healing" pyrrole based treatment of CdS/CdTe photovoltaics. *Sol Energy*

Mater Sol Cells. 2011;95(7):1716-1719. https://doi.org/10.1016/j.solmat.2011.01.038

223. Li Y, Li H, Zhong C, Sini G, Brédas J-L. Characterization of intrinsic hole transport in single-crystal spiro-OMeTAD. *npj Flexible Electronics*. 2017;1(1):2. https://doi.org/10.1038/s41528-017-0002-0

224. Li Z, Xiao C, Yang Y, et al. Extrinsic ion migration in perovskite solar cells. *Energy Environ Sci*. 2017;10(5):1234-1242. https://doi.org/10.1039/C7EE00358G

225. Du X, Chen Z, Liu F, et al. Improvement in open-circuit voltage of thin film solar cells from aqueous nanocrystals by interface engineering. *ACS Appl Mater Interfaces*. 2016;8(1):900-907. https://doi.org/10.1021/acsami.5b10374

226. Shalvey TP, Phillips LJ, Durose K, Major JD. A comparison of organic back contact materials for CdTe solar cells. In *2018 IEEE 7th World Conference on Photovoltaic Energy Conversion (WCPEC) (A Joint Conference of 45th IEEE PVSC, 28th PVSEC & 34th EU PVSEC)*. Waikoloa Village, HI: IEEE; 2018:846-851. https://doi.org/10.1109/PVSC.2018.8547725

227. Major JD, Phillips LJ, Al Turkestani M, et al. P3HT as a pinhole blocking back contact for CdTe thin film solar cells. *Sol Energy Mater Sol Cells*. 2017;172:1-10. https://doi.org/10.1016/j.solmat.2017.07.005

228. Wei H, Fang Y, Yuan Y, Shen L, Huang J. Trap engineering of CdTe nanoparticle for high gain, fast response, and low noise P3HT:CdTe nanocomposite photodetectors. *Adv Mater*. 2015;27(34):4975-4981. https://doi.org/10.1002/adma.201502292

229. Abdul-Manaf NA, Echendu OK, Fauzi F, Bowen L, Dharmadasa IM. Development of polyaniline using electrochemical technique for plugging pinholes in cadmium sulfide/cadmium telluride solar cells. *JEM*. 2014;43(11):4003-4010. https://doi.org/10.1007/s11664-014-3361-5

230. de Boer B, Hadipour A, Mandoc MM, van Woudenbergh T, Blom PWM. Tuning of metal work functions with self-assembled monolayers. *Adv Mater*. 2005;17(5):621-625. https://doi.org/10.1002/adma.200401216

231. Paudel NR, Yan Y. CdTe thin-film solar cells with cobalt-phthalocyanine back contacts. *Appl Phys Lett*. 2014;104(14):143507. https://doi.org/10.1063/1.4871093

232. Ke W, Zhao D, Grice CR, Cimaroli AJ, Fang G, Yan Y. Efficient fully-vacuum-processed perovskite solar cells using copper phthalocyanine as hole selective layers. *J Mater Chem A*. 2015;3(47):23888-23894. https://doi.org/10.1039/C5TA07829F

233. Varadharajaperumal S, Ilango MS, Hegde G, Satyanarayan MN. Effect of CuPc and PEDOT:PSS as hole transport layers in planar heterojunction CdS/CdTe solar cell. *Mater Res Express*. 2019;6(9):095009. https://doi.org/10.1088/2053-1591/ab2c61

234. Walkons C, Guralnick B, McCandless B, Birkmire R. CdTe Solar cells with a PCBM back contact. In: *2014 IEEE 40th Photovoltaic Specialist Conference (PVSC)*. Denver, CO: IEEE. 2014:1567-1572. https://doi.org/10.1109/PVSC.2014.6925217

235. Urieta-Mora J, García-Benito I, Molina-Ontoria A, Martín N. Hole transporting materials for perovskite solar cells: a chemical approach. *Chem Soc Rev*. 2018;47(23):8541-8571. https://doi.org/10.1039/C8CS00262B

236. Kim S, Jeon J, Suh J, et al. Comparative study of Cu_2Te and Cu back contact in CdS/CdTe solar cell. *J Kor Phys Soc*. 2018;72(7):780-785. https://doi.org/10.3938/jkps.72.780

237. Kindvall A, Munshi A, Shimpi T, Danielson A, Sampath WS. Copper-doped zinc telluride thin-films as a back contact for cadmium telluride photovoltaics. In: *2018 IEEE 7th World Conference on Photovoltaic Energy Conversion (WCPEC) (A Joint Conference of 45th IEEE PVSC, 28th PVSEC & 34th EU PVSEC)*. Waikoloa Village, HI: IEEE; 2018:2994-2997. https://doi.org/10.1109/PVSC.2018.8548102

238. Oklobia O, Kartopu G, Irvine SJC. *Arsenic – Doped p+-ZnTe Back Contact Films for CdTe Solar Cells; PVSAT*. London, UK: UCL; 2018:4.

239. Marsillac S, Parikh VY, Compaan AD. Ultra-thin bifacial CdTe solar cell. *Sol Energy Mater Sol Cells*. 2007;91(15–16):1398-1402. https://doi.org/10.1016/j.solmat.2007.04.025

240. Makhratchev K, Price KJ, Ma X,, et al. ZnTe:N back contacts to CdS/CdTe solar cells. In: *Conference Record of the Twenty-Eighth IEEE Photovoltaic Specialists Conference - 2000 (Cat. No.00CH37036)*. Anchorage, AK: IEEE; 2000:475-478. https://doi.org/10.1109/PVSC.2000.915874

241. Uličná S, Isherwood PJM, Kaminski PM, Walls JM, Li J, Wolden CA. Development of ZnTe as a back contact material for thin film cadmium telluride solar cells. *Vacuum*. 2017;139:159-163. https://doi.org/10.1016/j.vacuum.2017.01.001

242. Romeo N, Bosio A, Tedeschi R, Romeo A, Canevari V. A highly efficient and stable CdTe/CdS thin film solar cell. *Sol Energy Mater Sol. Cells*. 1999;58(2):209-218. https://doi.org/10.1016/S0927-0248(98)00204-9

243. Hodges DR. *Development of CdTe Thin Film Solar Cells on Flexible Foil Substrates*. PhD thesis. University of South Florida; 2009.

244. Hu S, Zhu Z, Li W, et al. Band diagrams and performance of CdTe solar cells with a Sb_2Te_3 back contact buffer layer. *AIP Adv*. 2011;1(4):042152. https://doi.org/10.1063/1.3663613

245. Emziane M, Durose K, Halliday DP, Bosio A, Romeo N. Efficiency improvement in thin-film solar cell devices with oxygen-containing absorber layer. *Appl Phys Lett*. 2005;87(26):261901. https://doi.org/10.1063/1.2152108

246. Zhang M-J, Lin Q, Yang X, et al. Novel P-type conductive semiconductor nanocrystalline film as the back electrode for high-performance thin film solar cells. *Nano Lett*. 2016;16(2):1218-1223. https://doi.org/10.1021/acs.nanolett.5b04510

247. Rockett A, Marsillac S, Collins R. *Novel Contact Materials for Improved Performance CdTe Solar Cells Final Report*; DE-EE0005405, 1433077; 2018; p DE–EE0005405, 1433077. https://doi.org/10.2172/1433077

248. Yang R, Wang D, Jeng M, Ho K, Wang D. Stable CdTe thin film solar cells with a MoO_x back-contact buffer layer. *Prog Photovolt Res Appl*. 2016;24(1):59-65. https://doi.org/10.1002/pip.2645

249. Wang D, Yang R, Wu L, Shen K, Wang D. Band alignment of CdTe with MoO_x oxide and fabrication of high efficiency CdTe solar cells. *Sol Energy*. 2018;162:637-645. https://doi.org/10.1016/j.solener.2018.01.031

250. Paudel NR, Compaan AD, Yan Y. Sputtered CdS/CdTe solar cells with $MoO_{3−x}$/Au back contacts. *Sol Energy Mater Sol Cells*. 2013;113:26-30. https://doi.org/10.1016/j.solmat.2013.01.041

251. Irfan I, Lin H, Xia W, Wu HN, Tang CW, Gao Y. The effect of MoO_x inter-layer on thin film CdTe/CdS solar cell. *Sol Energy Mater Sol Cells*. 2012;105:86-89. https://doi.org/10.1016/j.solmat.2012.04.006

252. Dang H, Singh VP. Nanowire CdS-CdTe solar cells with molybdenum oxide as contact. *Sci Rep*. 2015;5(1):14859. https://doi.org/10.1038/srep14859

253. Khrypunov MG, Kudii DA, Kovtun NA, Kharchenko MM, Khrypunova IV. Development of back and front contacts for CdTe layer in tandem flexible photoelectric converters on basis of CdTe/CuInSe₂. *Internat J Photoenergy*. 2019;2019:1-8. https://doi.org/10.1155/2019/9535123

254. Wu X, Zhou J, Duda A, et al. 13·9%-efficient CdTe polycrystalline thin-film solar cells with an infrared transmission of ∼50%. *Prog Photovolt Res Appl*. 2006;14(6):471-483. https://doi.org/10.1002/pip.664